

**EFFECT OF COMBINED UV AND FREE CHLORINE  
ON THE FORMATION OF  
CHLORONITROMETHANES**

A Thesis  
Presented to  
The Academic Faculty

by

David Vargas

In Partial Fulfillment  
of the Requirements for the Degree  
Masters of Science in the  
School of Civil and Environmental Engineering

Georgia Institute of Technology  
December 2015

**COPYRIGHT 2015 BY DAVID VARGAS**

**EFFECT OF COMBINED UV AND FREE CHLORINE ON THE  
FORMATION OF CHLORONITROMETHANES**

Approved by:

Dr. Ching-Hua Huang, Advisor  
School of Civil and Environmental Engineering  
*Georgia Institute of Technology*

Dr. Yongsheng Chen  
School of Civil and Environmental Engineering  
*Georgia Institute of Technology*

Dr. Spyros Pavlostathis  
School of Civil and Environmental Engineering  
*Georgia Institute of Technology*

Date Approved: 8/21/2015

To my parents, Heriberto and Maria Carmen Vargas, my siblings, Daisy and Roberto Vargas and all my family and friends who have helped and supported me throughout this process.

## **ACKNOWLEDGEMENTS**

I wish to thank Dr. Ching-Hua Huang, Dr. Spyros Pavlostathis, and Dr. Yongsheng Chen for serving as committee members and giving guidance. I'd also like to thank Wan-Ning Lee, Jie Fu, and the Huang research group for continuous help and feedback on my project. Finally, I'd like to thank the Vargas, Manriquez, and Servin family for support, and encouragement especially from my mother and father.

# TABLE OF CONTENTS

|  | Page |
|--|------|
| ACKNOWLEDGEMENTS                               | iv   |
| LIST OF TABLES                                 | vii  |
| LIST OF FIGURES                                | viii |
| LIST OF SYMBOLS AND ABBREVIATIONS              | x    |
| SUMMARY  | xii  |
| <u>CHAPTER</u>                                 |      |
| 1 Introduction                                 | 1    |
| 1.1 Disinfection Byproducts                    | 1    |
| 1.2 Combined UV/Cl <sub>2</sub> Systems        | 3    |
| 1.3 Precursors                                 | 5    |
| 1.4 Research Objectives                        | 6    |
| 2 Materials and Methods                        | 8    |
| 2.1 Chemicals and Samples                      | 8    |
| 2.2 Analytical Methods                         | 9    |
| 2.2.1 Calibration Standards                    | 9    |
| 2.2.2 Liquid-Liquid Extraction                 | 9    |
| 2.2.3 Analysis of Sample Water Characteristics | 10   |
| 2.2.4 Analysis of CNMs                         | 10   |
| 2.3 UV Experimental Setup and Sampling         | 10   |
| 2.3.1 Experimental Setup                       | 10   |
| 2.3.2 CNM Photostability                       | 12   |
| 2.4 Radical Quenchers                          | 13   |

|       |   |    |
|-------|---|----|
| 3     | Results and Discussion                                  | 14 |
| 3.1   | Enhanced HNM Formation                                  | 14 |
| 3.2   | Change in Cl:N Ratio                                    | 17 |
| 3.3   | HNM Stability   | 19 |
| 3.4   | Different Precursors                                    | 21 |
| 3.5   | Radical Quenchers                                       | 24 |
| 3.5.1 | <i>Tert</i> Butyl Alcohol                               | 24 |
| 3.5.2 | Sodium Acetate  | 27 |
| 3.5.3 | Nitrobenzene  | 28 |
| 3.6   | Real Water  | 30 |
| 3.6.1 | Wastewater Samples                                      | 30 |
| 3.6.2 | River Water Samples                                     | 32 |
| 3.6.3 | Partially Treated Drinking Water Samples                | 33 |
| 3.7   | Reaction Mechanisms                                     | 35 |
| 3.7.1 | Formation of HNMs by Chlorination                       | 35 |
| 3.7.2 | Formation of HNMs under Combined UV/Chlorine Conditions | 37 |
| 4     | Conclusion and Recommendations                          | 39 |
|       | REFERENCES  | 41 |

## LIST OF TABLES

|   |    |
|---|----|
| Table 1.1: Names, structures, molecular weights, and pKa of HNMs                  | 2  |
| Table 1.2: Names, structures, molecular weights and PKA of HNM Precursors         | 7  |
| Table 2.1: Water characteristics of collected water samples                       | 9  |
| Table 3.1: Reaction rate constants of HNMs with OH radical and hydrated electrons | 21 |
| Table 3.2: Lysine Peak Areas in the presence and absence of UV                    | 24 |

## LIST OF FIGURES

|  | Page |
|--|------|
| Figure 2.1: Schematic of UV chamber  | 12   |
| Figure 3.1: HNM formation from chlorination of MA in absence of UV exposure  | 15   |
| Figure 3.2: HNM formation from MA under combined UV/Cl <sub>2</sub> conditions   | 16   |
| Figure 3.3: FAC residual concentration over time in presence and absence of UV irradiation   | 16   |
| Figure 3.4: Maximum HNM concentration at 10 min of reaction time under combined UV/Cl <sub>2</sub> and using different Cl:N Ratios of free chlorine to MA. | 18   |
| Figure 3.5: Stability of HNMs in absence of UV   | 19   |
| Figure 3.6: Stability of HNMs in 2 mW/cm <sup>2</sup> of LPUV irradiance   | 20   |
| Figure 3.7: HNM formation from MA under combined UV/Cl <sub>2</sub> conditions   | 22   |
| Figure 3.8: HNM formation from DMA under combined UV/Cl <sub>2</sub> conditions  | 22   |
| Figure 3.9: HNM formation from Gly under combined UV/Cl <sub>2</sub> conditions  | 23   |
| Figure 3.10: HNM formation from MA under combined UV/Cl <sub>2</sub> conditions with the addition of 1 g/L TBA   | 25   |
| Figure 3.11: Total HNM, TCNM, and MCNM formation from MA under combined UV/Cl <sub>2</sub> conditions with the addition of various amounts of TBA          | 26   |
| Figure 3.12: HNM formation from MA under combined UV/Cl <sub>2</sub> conditions with the addition of 1 g/L sodium acetate                                  | 28   |
| Figure 3.13: HNM formation from MA under combined UV/Cl <sub>2</sub> conditions with the addition of 0.05 g/L NB   | 29   |
| Figure 3.14: HNM formation under combined UV/Cl <sub>2</sub> conditions with the addition of 0.05 g/L NB   | 29   |
| Figure 3.15: HNM formation from a wastewater sample under combined UV/Cl <sub>2</sub> conditions   | 31   |
| Figure 3.16: HNM formation from a wastewater sample and spiked MA under combined UV/Cl <sub>2</sub> conditions   | 31   |
| Figure 3.17: HNM formation from a river sample under combined UV/Cl <sub>2</sub> conditions  | 32   |



|   |    |
|---|----|
| Figure 3.18: HNM formation from a river sample and spiked MA under combined UV/Cl <sub>2</sub> conditions                             | 33 |
| Figure 3.19: HNM formation from a partially treated drinking water sample under combined UV/Cl <sub>2</sub> conditions                | 34 |
| Figure 3.20: HNM formation from a partially treated drinking water sample with spiked MA under combined UV/Cl <sub>2</sub> conditions | 34 |

## LIST OF SYMBOLS AND ABBREVIATIONS

|                               |   |
|-------------------------------|---|
| Cl•                           | Chlorine Atom                                   |
| Cl:N                          | Chlorine to Nitrogen Ratio                      |
| CNM                           | Chloronitromethane                              |
| DBPs                          | Disinfection Byproducts                         |
| DCNM                          | Dichloronitrmethane                             |
| DI                            | Deionized                                       |
| DMA                           | Dimethylamine                                   |
| DON                           | Dissolved Organic Nitrogen                      |
| DO                            | Dissolved Oxygen                                |
| DPD                           | <i>N,N</i> -diethyl- <i>p</i> -phenylenediamine |
| FAC                           | Free Available Chlorine                         |
| GC/ECD                        | Gas Chromatography-electron capture device      |
| Gly                           | Glycine   |
| HAA                           | Haloacetic Acid                                 |
| HNM                           | Halonitrmethane                                 |
| LLE                           | Liquid-Liquid Extraction                        |
| Lys                           | Lysine  |
| LPUV                          | Low Pressure Ultraviolet                        |
| MA                            | Methylamine                                     |
| MCNM                          | Monochloronitrmethane                           |
| MPUV                          | Medium Pressure Ultraviolet                     |
| MTBE                          | Methyl tert-butyl ether                         |
| N <sub>2</sub> O <sub>4</sub> | Dinitrogen tetroxide                            |

|                   |                                    |
|-------------------|------------------------------------|
| NB                | Nitrobenzene                       |
| N-DBP             | Nitrogenous Disinfection Byproduct |
| NO•               | Nitric Acid                        |
| NO <sub>2</sub> • | Nitrogen Dioxide                   |
| NOM               | Natural Organic Matter             |
| OH•               | Hydroxyl Radical                   |
| TBA               | <i>Tert</i> -Butyl Alcohol         |
| TCNM              | Trichloronitrmethane               |
| THM               | Trihalomethane                     |
| TOC               | Total Organic Carbon               |
| TON               | Total Organic Nitrogen             |
| TN                | Total Nitrogen                     |

## SUMMARY

The results from this study show how different precursors affect halonitromethane (HNM) formation as well as how different free chlorine doses can affect HNM speciation. This study shows that the low pressure ultraviolet (LPUV) and free chlorine concurrent exposure can enhance HNM formation. In addition, most previous studies in the literature showed trichloronitromethane (TCNM) forming in greater quantities followed by monochloronitromethane (MCNM) and dichloronitromethane (DCNM). However, the results of this study show that, in deionized (DI) water matrices, MCNM forms in greater quantities at chlorine to nitrogen (Cl:N) ratios less than 3, while TCNM forms in greater quantities at Cl:N ratios greater than 3. Even so, the increase in TCNM formation did not increase linearly as the Cl:N ratio increased; there was a decreased rate of return when Cl:N ratios were greater than 3. The type of nitrogenous precursors can affect the amount of HNMs formed, with glycine forming a higher amount of total HNMs compared to methylamine (MA) and dimethylamine (DMA). The source of water can also affect which HNM species is formed in greater concentrations. The limited number of real water samples showed that the river waters have higher than normal total organic carbon (TOC) and dissolved organic nitrogen (DON), which are associated with greater nitrogenous precursors and higher HNM formation. Each water source can have different nitrogenous precursors; river waters may have more algal organic matter while wastewater would have higher organic matter and synthetic chemicals. In addition, source waters can have different constituents, such as varying dissolved oxygen (DO) levels and inorganic ions, which might inhibit HNM formation or affect specification.

# CHAPTER 1

## INTRODUCTION

### 1.1 Disinfection Byproducts

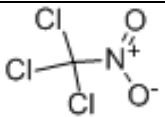
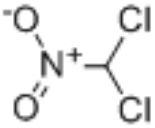
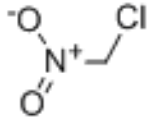
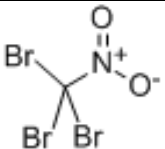
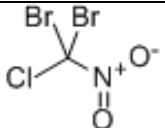
In water treatment, the disinfection process involves adding an oxidant to remove any pathogens before consumption. Such oxidants can include chlorine, chloramine, ozone, or ultraviolet exposure (Mincher et al. 2010). If there is any natural organic matter (NOM) present in the water, the oxidants can react with NOM, creating disinfection byproducts (DBPs). One of the first classes of DBPs to be identified and regulated were the trihalomethanes (THMs) and haloacetic acids (HAAs), which are also the most common DBPs found in the drinking water surveys conducted in the United States (Pontius et al. 1990, Krasner et al. 2006).

Regulated DBPs have been extensively studied due to their prevalence and can form in concentrations ranging from 1 to 100 µg/L and are associated with bladder and rectal cancers as well as reproductive issues (Nieuwenhuijsen et al. 2000). The main precursors of THMs and HAAs are natural organic matter found in the source waters (Cantor 1996). In an effort to reduce regulated DBPs, different disinfection methods are sought out such as ozonation/chlorination, and combined UV/chlorination. However, these alternatives can contribute to the formation of nitrogenous disinfection byproducts (N-DBPs) (Bond et al. 2011). Some examples of N-DBPs include haloacetoneitriles, nitrosamines, and halonitroalkanes (Mitch et al. 2009).

Halonitromethanes (HNMs) are a type of halonitroalkane and contain a nitro group and up to three halogens on the  $\alpha$ -carbon (Shah et al. 2012). Examples of HNMs (Table 1.1) include monochloronitromethane (MCNM), dichloronitromethane (DCNM), trichloronitromethane (TCNM or chloropicrin), bromochloronitromethane, bromopicrin, and other nitromethanes with mixed halogens, such as Cl or Br, on the methyl carbon.

TCNM was not officially recognized as a DBP until 1988 in the Drinking Water Priority List of 1988 (Pontius et al. 1990). These HNMs tend to form in waters treated with ozonation followed by chlorination or chloramination (Plewa et al. 2004).

**Table 1.1:** Names, structures, molecular weights, and pKa of HNMs.

| Name  | Structure   | MW (g/mol) | pKa  |
|---|---|------------|------|
| Trichloronitromethane (TCNM) (Chloropicrin) |    | 164.38     | NA   |
| Dichloronitromethane (DCNM)                 |    | 129.93     | 5.97 |
| Monochloronitromethane (MCNM)               |    | 95.49      | 7.0  |
| Bromopicrin                                 |   | 297.72     | NA   |
| Dibromochloronitromethane                   |  | 253.27     | NA   |

Currently, many N-DBPs are known to be even more genotoxic and cytotoxic compared to the regulated DBPs (HNMs and HAAs) and form in water and wastewater treatment. For example, DCNM can form at 1/27<sup>th</sup> of the concentration of chloroacetic acid found but is known to be at least 30 times greater in cytotoxicity (Plewa et al. 2004). Additionally, the brominated HNMs can be more toxic than the solely chlorinated ones, with dibromonitromethane being the most toxic due to the high reactivity of the nitro group (Hu et al. 2010b). Some studies have suggested an association of exposure to DBPs in drinking water with bladder cancer, while others countered that there were no

identified DBPs yet that were believed to be bladder carcinogens (Villanueva et al. 2007, Hrudey et al. 2009, Bond et al. 2011).

The different forms of chloronitromethane (CNMs) vary by the degree of chlorination, ranging from mono-, di-, and trichloronitromethane (MCNM, DCNM, TCNM). The most commonly detected form of HNM is TCNM followed by MCNM, and then DCNM (Weinberg et al. 2002, Richardson et al. 2007, Fang et al. 2013).

## **1.2 Combined UV/Cl<sub>2</sub> systems**

In North America, UV light is applied for drinking water to reduce the level of chlorinated DBPs formation and aid in control of chlorine-resistant microorganisms by damaging DNA material in the microorganisms (Deng et al. 2014). The UV process can use two types of lamps, medium pressure and low pressure UV lamps. Medium pressure UV (MPUV) lamps emit light from 200-400 nm whereas low-pressure (LPUV) lamps emit monochromatically at 254 nm (Shah et al. 2012). A nationwide survey reports that 62% of water treatment facilities use MPUV while 28% use LPUV, and the secondary disinfectant of choice was typically chlorine, rather than chloramine (Dotson et al. 2012, Lyon et al. 2012). Organic matter can absorb UV light in the 200-400 nm wavelengths. The high molecular-weight organic matter in NOM is decomposed to low molecular weight organic acids by UV irradiation and can be further mineralized to carbon dioxide or react with other chemicals in the waters (Corin et al. 1996). However, a secondary disinfectant (e.g. free chlorine) is usually added post UV treatment to keep a residual disinfectant in the distribution systems (Craik et al. 2001, Hijnen et al. 2006, Weng et al. 46).

In a combined UV/Cl<sub>2</sub> system, UV photolysis of HOCl and OCl<sup>-</sup> can produce both hydroxyl radical (OH•) and chlorine atom (Cl•), with OH• being the predominant radical species (Feng et al. 2007, Bolton et al. 2010, Jin et al. 2011). This can weaken the photolysis of other substances that may be present in the water (Watts et al. 2007),

however, does not reduce the efficacy of removing chlorine resistant bacteria, bacteriophages, and enteroviruses compared to UV light exposure alone (Montemayor et al. 2008). When the UV/Cl<sub>2</sub> system reactions are dominant, the water is in a highly photocatalyzed oxidative state (Korshin et al. 2007, Liu et al. 2012) and form an advanced oxidation process that can help break down other organic matter (Deng et al. 2014).

The irradiation of LPUV lamps has a small overlap with nitrite's absorbance band, while the irradiation of MPUV lamps overlaps with both the absorbance bands of nitrite and nitrate greatly. As a result, MPUV lamps followed by postchlorination can increase HNM formation by as much as 200% compared to chlorination alone. In MPUV, TCNM formation increases 6 folds compared to similar conditions under LPUV (Shah et al. 2012). However, UV irradiation alone has minimal impact on the regulated DBPs mentioned earlier (Lyon et al. 2012).

Previous research (Deng et al. 2014) examined the enhanced formation of TCNM from polyamine, dimethylamine, and methylamine under combined LPUV/Cl<sub>2</sub> and witnessed these abundant chemicals can serve as TCNM precursors. Additionally, Shah et al. (2012) observed an enhanced TCNM formation from MPUV/post chlorination of nitrate-rich waters, and the TCNM formation was doubled in prechlorination/MPUV systems compared to postchlorination.

The combined UV/Cl<sub>2</sub> system can be found in chlorinated swimming pools, as UV light is also applied in swimming pools, primarily for destruction of volatile chloramines that are harmful to human health (Li et al. 2009), as well as in homes that have residual chlorine from drinking plants and use additional UV disinfection.



### 1.3 Precursors

Because the N-DBPs contain at least one or more nitrogen atom(s), their precursors are expected to be organic nitrogen-containing compounds. Nitrogenous organic precursors tend to be hydrophilic, have a low molecular weight, and lack an electrostatic charge in waters (Bond et al. 2012). Some examples include free amino acids, such as glycine, nucleic acids, amino sugars, proteins, and any other type of dissolved organic nitrogen (DON) (Westerhoff and Mash 2002, Shah et al. 2012). A higher concentration of DON, which commonly originates from algal organic matter or biopolymers from wastewater effluents, is correlated to higher N-DBP formation. (Westerhoff and Mash 2002, Bond et al. 2012). Such findings also suggest the nitrogen source of N-DBPs is from NOM rather than external inorganic sources such as nitrite and nitrate (Bond et al. 2012).

The nitrogenous precursors' hydrophilic nature and lack of charge can cause resistance in their removal through conventional water and wastewater treatment processes such as coagulation and filtration (Mitch et al. 2009, Bond et al. 2012). An alternative to eliminate nitrogenous precursors would be bioremediation or nanofiltration (Bond et al. 2012, Shah et al. 2012). To date, literature shows that there are still many unidentified N-DBP precursors in natural waters (Bond et al. 2012).

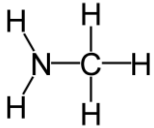
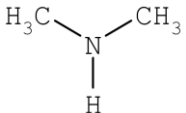
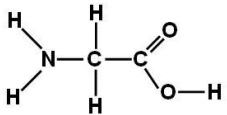
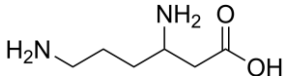
From chlorination alone, the major CNM formation pathway is through the initial formation of a nitroalkane, followed by sequential chlorine addition to the  $\alpha$ -carbon. The nitro group increases the acidity of the C-H bond allowing halogenation of the compound to be favorable (Shah et al. 2012). The rate-limiting step is the deprotonation of the  $\alpha$ -carbon, which increases with more chlorines attached and is favored at higher pH (Shah et al. 2012). The typical yields of CNM formation by chlorination or chloramination ranged from 0.01% to 0.08%. Another formation pathway of CNMs involve the chlorination of nitrite, forming nitrating agents, such as  $\text{ClNO}_2$ , and  $\text{N}_2\text{O}_4$ , which can help introduce nitro groups to organic compounds (Shah et al. 2012).

Nitrite and nitrate, when present in water, can absorb UV light in the <250 nm and 270 to 400 nm wavelengths, respectively, and form nitric oxide (NO<sup>•</sup>), hydroxyl radicals (OH<sup>•</sup>), and nitrating agents such as nitrogen dioxide (NO<sub>2</sub><sup>•</sup>) and dinitrogen tetroxide (N<sub>2</sub>O<sub>4</sub>) (Shah et al. 2012). These reactive nitrogen species can promote the nitration of NOM, which can also enhance HNM formation with chlorination especially in MPUV/Cl<sub>2</sub> systems as described earlier.

#### **1.4 Research Objectives**

The objective of this study was to develop a better understanding of how the formation of CNM DBPs is affected when combined UV/Cl<sub>2</sub> conditions are employed in water treatment. Particularly, this study evaluated the formation and distribution of MCNM, DCNM and TCNM from several different nitrogenous precursors in clean and real water matrices under combined UV/Cl<sub>2</sub> conditions, and compared that with the formation of CNMs by chlorination only. The studied nitrogenous precursors included methylamine (MA), dimethylamine (DMA), glycine (Gly), and lysine (Lys) (Table 1.2). These alkylamines and amino acids were selected because they are common DON compounds in source waters and have been shown to be TCNM precursors (Deng et al 2014, Shan et al. 2012). LPUV was chosen as the light source in this study because limited research is available thus far on the effect of LPUV on the combined UV/chlorination systems with regards to DBP issues.

**Table 1.2:** Names, structures, molecular weights, and pKa of HNM precursors. pKa for Gly and Lys represent carboxyl side and amine side respectively

| Name                | Structure  | MW     | pKa       |
|---------------------|--|--------|-----------|
| Methylamine (MA)    |   | 31.06  | 10.66     |
| Dimethylamine (DMA) |   | 87.12  | 10.73     |
| Glycine (Gly)       |   | 75.06  | 2.31/9.78 |
| Lysine (Lys)        |  | 146.19 | 2.16/9.06 |

## CHAPTER 2

### MATERIALS AND METHODS

#### 2.1 Chemicals and Samples

Standard grade MCNM, DCNM, and TCNM were purchased from Cansync Chemical Corporation at 90-95+% purity. Methyl *tert*-butyl ether (MTBE), methylamine hydrochloride, dimethylamine hydrochloride, monobasic and dibasic sodium phosphate, sodium sulfate, hydrochloric acid, sodium hydroxide, sodium thiosulfate, ferrous ammonia sulfate, *N,N*-diethyl-*p*-phenylenediamine (DPD), sodium hypochlorite, glycine and lysine were purchased from Sigma Aldrich or Fisher Scientific at >98% purity. Deionized water (DI) was produced via Millipore Milli-Q water purification system. Waters from a domestic wastewater treatment plant, a drinking water treatment plant, and the Chattahoochee River were collected. Wastewater was collected after conventional nitrification, denitrification, and phosphorus removal processes, followed by membrane filtration and prior to any disinfection. Drinking water was collected after coagulation and flocculation and prior to any disinfection. River water was collected directly from the Chattahoochee River. Table 2.1 below outlines water characteristics of the collected water samples.

Table 2.1: Water characteristics of collected water samples, n=1

|   | Wastewater | Drinking Water | River Water |
|---|------------|----------------|-------------|
| TN (mg-N/L)                               | 7.64       | 0.40           | 0.98        |
| Nitrate (mg-N/L)                          | 5.58       | 0.238          | 0.66        |
| Nitrite(mg-N/L)                           | 0.0006     | 0.0014         | 0.0014      |
| Ammonia(mg-N/L)                           | 0.0072     | 0.0017         | 0.0036      |
| TON (mg-N/L)                              | 2.05       | 0.16           | 0.315       |
| TOC (mg/L as C)                           | 10.25      | 3.07           | 3.717       |
| Abs UV <sub>254</sub> (cm <sup>-1</sup> ) | 0.127      | 0.069          | 0.050       |
| SUVA (mg/(L*cm))                          | 0.012      | 0.022          | 0.013       |

## 2.2 Analytical Methods

### 2.2.1 Calibration Standards

Calibration standards of each CNM (i.e., MCNM, DCNM and TCNM) were made with concentrations ranging from 0.1 to 15 µg/L. A liquid-liquid extraction (LLE) method was typically used to extract CNMs from water samples for analysis by gas chromatography/electron capture detector (GC/ECD). Thus, the calibration standards were prepared by dissolving a known amount of pure CNM liquid in water and serial dilution and then extracting by the LLE procedure, so that the recovery and extraction efficiency were taken into account in the calibration curve.

### 2.2.2 Liquid-Liquid Extraction

A 10 mL glass vial with 0.8 g of Na<sub>2</sub>SO<sub>4</sub> to increase MTBE separation in the LLE process (Huang et al. 2013) and 1 mL of 15 mM sodium thiosulfate for excess free

chlorine quenching were used in the LLE. The LLE procedure involved adding 1.7 mL of MTBE to 5 mL of aqueous reaction sample in the vial and shaking for 4 min, followed by extracting the MTBE layer from the sample vial to a 2-mL amber glass GC vial. Afterwards, the samples were analyzed by GC/ECD.

### **2.2.3 Analysis of Sample Water Characteristics**

TOC analysis was determined via a TOC-L analyzer (Shimadzu Corporation, Kyoto Japan). Nitrate nitrogen ( $\text{NO}_3\text{-N}$ ) and Nitrite-nitrogen ( $\text{NO}_2\text{-N}$ ) were analyzed by a DX-600 ion chromatography system (Dionex, Sunnyvale, California, USA).  $\text{NH}_4\text{-N}$  was measured with an Orion High-Performance Ammonia Electrode (Thermo Scientific, Waltham, Massachusetts, USA). Total nitrogen (TN) analysis was analyzed via a TOC/TN analyzer ((Shimadzu Corporation, Kyoto Japan). Free chlorine was determined by both DPD ferrous titrimetric method and DPD colorimetric method (Standard Methods 4500-Cl F. and 4500-Cl G.).

### **2.2.4 Analysis of CNMs**

The CNM concentrations were analyzed by an Agilent 6890 gas chromatography system with a HP-5MS capillary column (30 m x 250  $\mu\text{m}$  x 0.25 mm) and an electron capture detector (Palo Alto, CA). Calibration standards of CNMs (0.1-15  $\mu\text{g/L}$ ) yielded strong linear correlations ( $R^2 > 0.99$ ). The detection limit was around 0.1  $\mu\text{g/L}$  for all CNMs with an extraction efficiency ranging from 80-95%. Methods were adapted from the EPA method 551 (Hodgeson et al. 1990).

## **2.3 UV Experimental Setup and Sampling**

### **2.3.1 Experimental Setup**

Unless otherwise stated, a 100-mL cylindrical quartz reactor was filled with 80 mL of DI water and was magnetically stirred. To control pH, 2 mM phosphate buffer was added to the reactor and the pH was further adjusted with small quantities of 0.1 mM NaOH and HCl to 7.00, and then 73  $\mu$ M of MA or other model precursor was added. Free chlorine (from NaOCl solution) was then added at various concentration ranging from 5.17 to 51.7 mg/L (corresponding to chlorine to precursors Cl:N molar ratios of 1:1 to 10:1) and the reactor immediately placed in a UV chamber (Figure 2.1) to be exposed to UV irradiation. The UV reactor setup is similar to that described in Deng et al. (2014). UV irradiation was supplied from one side of the quartz reactor by typically one 4-W LP lamp (G4T5 Hg lamps, Philips TUV4W) peaking at 254 nm. The photochamber was equipped with a fan for cooling during the experiments (near room temperature at  $\sim 22^{\circ}\text{C}$ ). The UV lamps were allowed to warm up for at least 15-20 min prior to the experiment. The incident light irradiance to the quartz reactor center was determined to be  $2.0 \text{ mW/cm}^2$  (corresponding to a photo fluence rate of  $3.36 \text{ mEinstein/L-s}$ ) by a UVX (UVP, USA) radiometer. Select experiments were conducted with two or three 4-W LP lamps, similar to the conditions in Deng et al. (2014). A 5-mL aliquot sample was taken at predetermined time intervals from the photoreactor and placed in a 10-mL glass vial which contained 1 ml of 15 mM sodium thiosulfate for immediate free chlorine quenching followed by LLE. Parallel experiments were conducted with the addition of free chlorine only but without UV exposure for comparison to assess the enhancement effect of combined UV/ $\text{Cl}_2$  on the CNMs' formation.

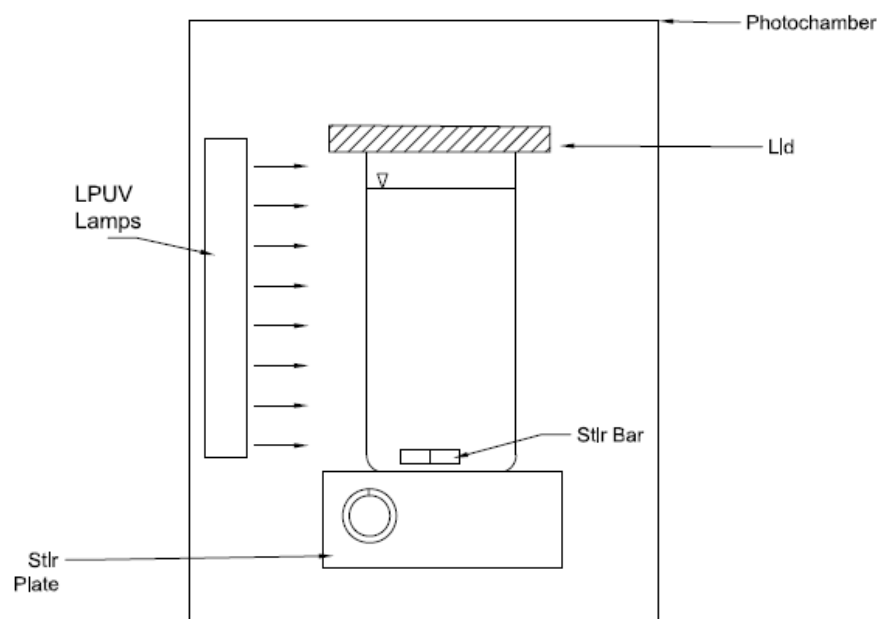


**Figure 2.1:** Schematic of UV chamber used in experimental set-up. The 80 mL quartz reactor has an approximate 2.75 cm diameter and 10 cm height. Up to three LPUV lamps in parallel were used. The top side of the chamber has access for sampling.

For experiments in the real water samples, the water samples were used as is or spiked with the model nitrogenous precursor and exposed to the combined UV/Cl<sub>2</sub> conditions as described above. The results of CNM formation under combined UV/Cl<sub>2</sub> were compared to the results from similar experiments but with chlorination only and without UV exposure.

### 2.3.2 CNM Photostability

To investigate the stability of CNMs under LPUV, each CNM was spiked at 5 µg/L in DI water matrix without any addition of free chlorine or other precursors and tested for its stability under LPUV exposure with the same experimental setup as that described in Section 2.3.1.



## 2.4 Radical Quenching

Three types of radical quenchers were used to determine the effects of radicals on CNM formation. *Tert*-butyl alcohol (TBA) was selected due to its high reactivity with OH• and Cl• (Gilbert et al. 1988). Nitrobenzene (NB) is known to react with OH• but not Cl• (Watts et al. 2007). Acetate anion reacts with Cl• ( $k = 3.7 \times 10^9 \text{ M}^{-1}\text{s}^{-1}$ ) about 50 times faster than with OH• ( $k = 7.5 \times 10^7 \text{ M}^{-1}\text{s}^{-1}$ ) (Buxton et al. 2000). In the radical quenching experiments, the experimental setup described earlier was used (73  $\mu\text{M}$  MA and 7.75 mg/L free chlorine) and the results with and without addition of radical quencher were compared. Unless specified otherwise, TBA, or sodium acetate was added at 1 g/L while NB was added at 0.05 g/L. As before, 5 ml sample aliquots were taken from the UV reactor at predetermined time intervals for analysis. The experiments using nitrobenzene as a OH• scavenger discovered that nitrobenzene could be a precursor to form CNMs under the combined UV/Cl<sub>2</sub> conditions and the results are also reported.

## CHAPTER 3

### RESULTS AND DISCUSSION

#### 3.1 Enhanced HNM Formation

Similar experiments of chlorination of MA (pH 7 by 2 mM phosphate buffer, 5.1 mg/L free chlorine, and 73  $\mu$ M MA or other precursors (Cl:N = 1:1)) were conducted in the presence and absence of UV to assess how the simultaneous exposure to UV and chlorine affect HNM formation. Figures 3.1 and 3.2 show the results from these experiments.

When MA was exposed to free chlorine alone, a small amount of HNMs formed throughout the experiment, with the highest abundant species, DCNM, peaking at 2.18 nM. In contrast, when MA was exposed to both free chlorine and UV, there was a 25 fold increase in MCNM formation, increasing from 0.8 nM to 20.3 nM. This 20+ fold increase suggests UV does enhance HNM formation. In addition, the peak total HNM concentration increased from 3.02 nM to 24.25 nM, an 8 fold increase. Note that the total HNM here refers to the total sum of MCNM, DCNM and TCNM concentrations. Because the experiments were conducted with little bromide present, brominated nitromethanes were expected to be of little significance. Free available chlorine (FAC, i.e., sum of HOCl and OCl<sup>-</sup>) consumption was found to behave differently under the two different conditions as shown in Figure 3.3. In the absence of UV, FAC was partially consumed within 5 min and remained stable after 7 min, with little to no consumption afterwards. In the presence of UV, FAC was consumed rapidly and completely within 5 min. The complete consumption of FAC at 5 min corresponded to the peak total HNM concentration in Figure 3.2, suggesting that once FAC was consumed, no additional

HNM could form and could undergo photo-decay. In addition, these results suggested that LPUV enhanced formation of each HNM species differently since the increase was variable for each respective HNM species. The HNM concentration at  $t=0$  may be attributed to the fast HNM formation between initial chlorine dose and sampling.

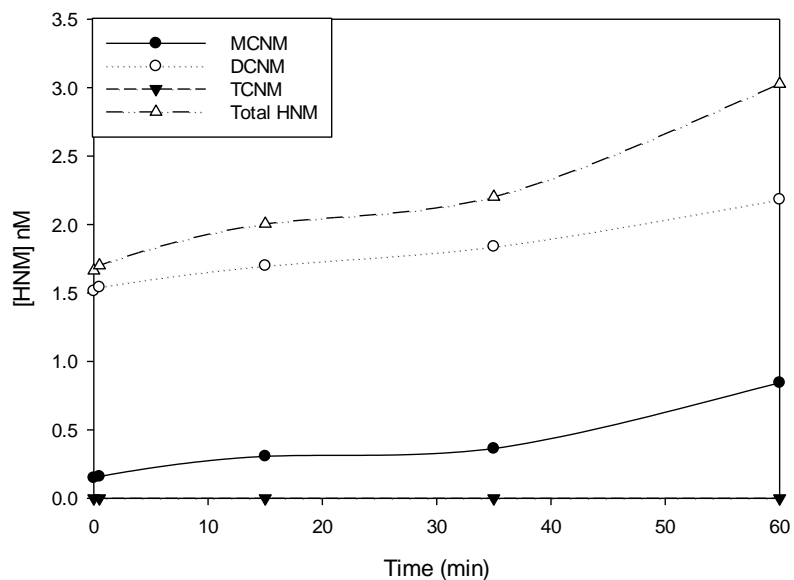


**Figure 3.1:** HNM formation from chlorination of MA in the absence of any LPUV exposure.  $[MA]_0=73 \mu\text{M}$ ,  $[FAC]_0= 5.17 \text{ mg/L}$  pH 7.0, and  $22^\circ\text{C}$ .  $n=1$

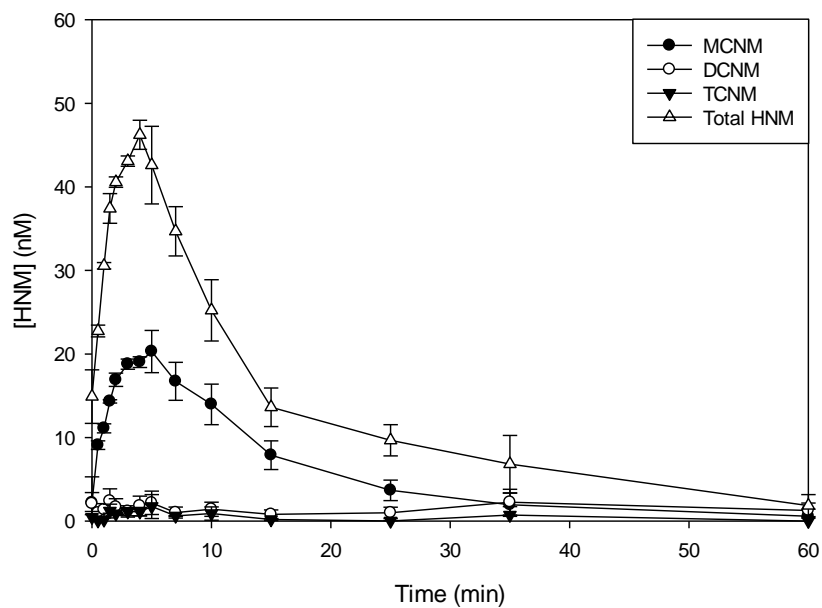


**Figure 3.2:** HNM formation from MA under combined UV/Cl<sub>2</sub> conditions. [MA]<sub>0</sub>=73 μM, [FAC]<sub>0</sub>= 5.17 mg/L, 2 mW/cm<sup>2</sup> LPUV exposure, pH 7.0, and 22 °C. Error bars are standard deviation, n=2.

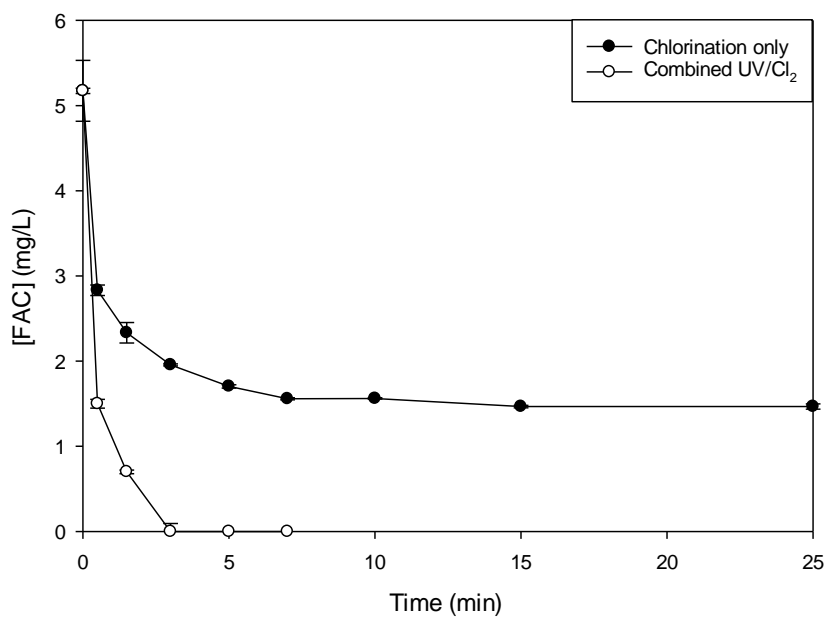


**Figure 3.3:** FAC residual concentration over time in the presence and absence of UV irradiation. Reaction conditions are the same as Figures 3.1 and 3.2, n=1.

Previous research has shown similar enhancement effect by combined UV/Cl<sub>2</sub> conditions with respect to TCNM formation from simple amines and polyamine precursors (Deng et al 2014). In the above study, somewhat different reaction conditions from the current study were employed: 10 mg/L of MA, DMA of polyamine and 7 mg/L FAC (Cl:N = 0.73 for the case of MA) at pH range of 6-8 and UV irradiance of 5.4 mW/cm<sup>2</sup>. The authors monitored only TCNM and observed its maximum concentration at reaction time of 3 min, compared to the reaction time of 5 min in the current study (Figure 3.2). The work by Deng et al. (2014) showed a 10+ fold increase in TCNM formation by combining UV and chlorine together. The results in this study from Figures 3.1-3.3 show a max formation yield of 0.03%, 0.003%, and 0.002% for MCNM, DCNM and TCNM, respectively. Past studies have mainly focused on TCNM and did not include MCNM and DCNM formation in their monitoring, showing the typical yields of TCNM ranging from 0.01% to 0.08% M (Shah et al 2012).

### **3.2 Change in Cl:N Ratio**

Because MCNM, DCNM and TCNM involve different levels of chlorination in their formation, different chlorine to nitrogen precursor (Cl:N) molar ratios in reaction conditions were tested. Figure 3.4 shows the concentrations of HNMs at reaction time of 10 min, which was on average that time the maximum total HNM concentration peaked. At low levels of chlorination, MCNM formed in greater quantities; however, higher chlorination levels corresponded to higher formation of TCNM compared to MCNM and DCNM. Meanwhile, DCNM formation remained relatively low compared to both MCNM and TCNM. The shift to TCNM predominance from MCNM predominance occurred when the Cl:N molar ratio was greater than 3.

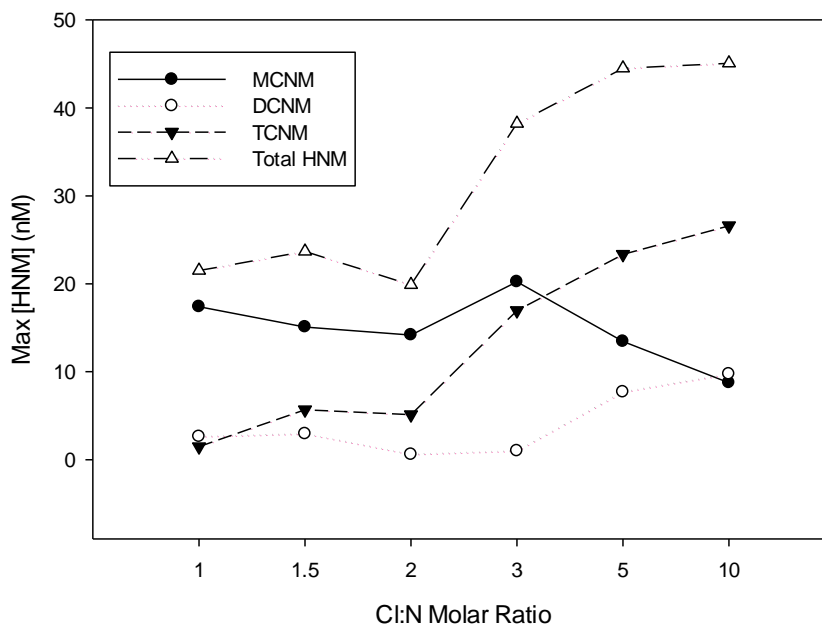


**Figure 3.4:** Maximum HNM concentration at 10 min of reaction time under combined UV/Cl<sub>2</sub> and using different Cl:N ratios of free chlorine to MA. At the employed Cl:N ratios, the maximum HNM concentration was at around 5 min, and already experienced some photolysis, n=1

To the author's knowledge, this is one of the first studies that compared MCNM, DCNM, and TCNM formation by a combined UV/Cl<sub>2</sub> system under different reaction conditions. Past research has stated that TCNM was found in greater concentrations compared to the other HNMs (Weinberg et al 2002, Richardson et al 2007, Fang et al 2013). In chlorination, the rate limiting-step in HNM formation is the initial chlorination (Shah et al 2012). Constituents in water that react with chlorine with faster kinetics can consume the FAC before the initial formation of HNMs, reducing the available chlorine for transformation of MCNM to TCNM. At higher chlorine doses, the excess chlorine allows for increased TCNM formation.

### 3.3 HNM Stability

After spiking 5  $\mu\text{M}$  of each individual HNM into the experimental setup, the reactor was kept in the dark or exposed to UV to determine how stable the HNMs were in the experimental conditions. Figure 3.5 shows that HNMs were stable in the absence of UV. The drop in HNM concentration was likely due to (i) small volatilization despite the reactor being covered; and (ii) extraction efficiencies. Figure 3.6 shows the rapid drop in HNM concentration when exposed to UV. DCNM photodecayed the fastest, followed by MCNM, and TCNM.

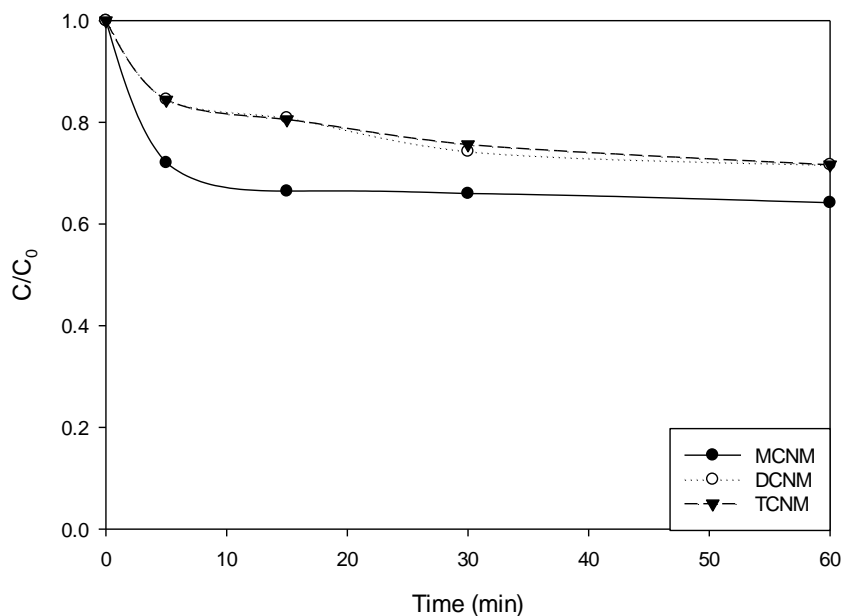


**Figure 3.5:** Stability of HNMs in the absence of UV.  $C_0 = 5.0 \mu\text{g/L}$ ,  $\text{pH} = 7.0$  by 2 mM phosphate buffer, and  $22^\circ\text{C}$ ,  $n=1$ .

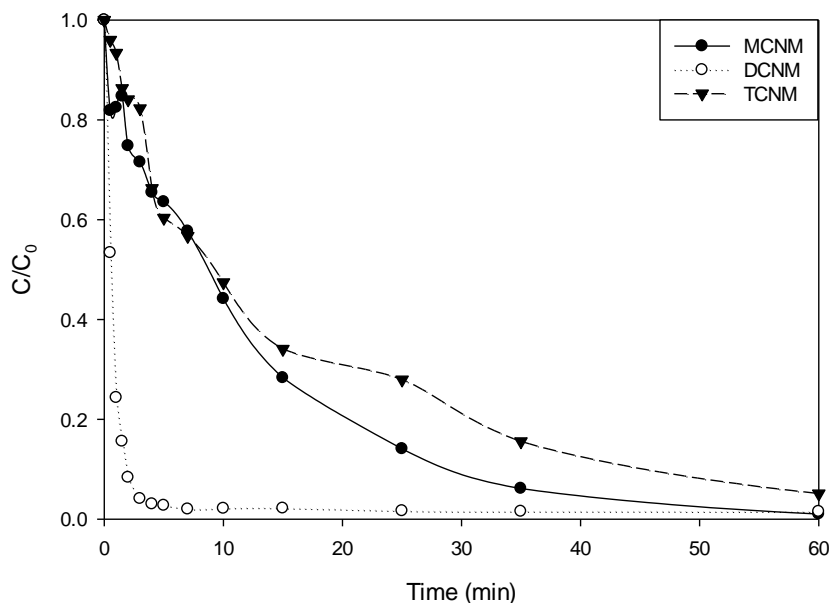


**Figure 3. 6:** Stability of HNMs at 2 mW/cm<sup>2</sup> of LPUV irradiance. C<sub>0</sub>= 5.0 µg/L, pH=7.0 in 2 mM phosphate buffer, and 22 °C, n=1

In the absence of UV, the stability of HNMs is consistent with the literature (Fang et al 2013). The drop in HNM concentration shown in Figure 3.5 suggested a small loss due to volatilization and/or lower than 100% of extraction efficiency. However, throughout the reaction process, the reactor and sample vials were all covered with a type of lid to minimize volatilization. In addition, the calibration curve was conducted from standards prepared in water with extraction to account for extraction efficiencies.

In UV light, photolysis can occur via direct photolysis and indirect photolysis. Fang et al. (2013) reported that photolysis of HNMs under LPUV lamps followed first-order rate kinetics. DCNM photolysis rates are pH dependent, increasing with pH, especially near its pK<sub>a</sub>. TCNM photolysis rates are independent of pH change and are relatively low at all pH ranges (Fang et al 2013). The degradation rates of DCNM were much faster than TCNM. Photolysis of HNMs was associated with an increase in chloride, nitrite and smaller amounts of nitrate (Fang et al 2013). The sudden drop of



DCNM in Figure 3.6 is in agreement with literature reports that DCNM has the fastest photo-decay kinetics under LPUV conditions.

HNMs may also be degraded by indirect photolysis through OH radicals reacting with HNMs and cleaving the C-N bond (Fang et al 2013). Hydrated electrons can also react with the  $\alpha$ -carbon to release halide or nitrite ions (Mezyk 2006, Cole et al 2007, Mincher et al 2009). However, hydroxyl radicals are relatively low in concentration, at  $10^{14}$  to  $10^{12}$  M, while hydrated electrons are consumed by dissolved oxygen in natural waters (Fang et al 2013). Table 3.1 shows the reported rate constants of HNMs with hydroxyl radicals and hydrated electrons (Mezyk et al 2006).

**Table 3.1:** Reaction rate constants of HNMs with OH $\cdot$  and hydrated electrons (Mincher et al 2010).

| Compound | Hydrated electron rate constant (M s) $^{-1}$ | OH RXN Rate constant (M s) $^{-1}$ |
|----------|---|------------------------------------|
| TCNM     | $2.13 \times 10^{10}$                         | $4.84 \times 10^7$                 |
| DCNM     | $3.21 \times 10^{10}$                         | $5.12 \times 10^8$                 |
| MCNM     | $3.01 \times 10^{10}$                         | $1.94 \times 10^8$                 |

### 3.4 Different Precursors

Four different nitrogenous precursors, MA, DMA, glycine, and lysine, were compared for their potential to form HNMs under combined UV/Cl $_2$  conditions. Each precursor was exposed to a chlorine dose corresponding to a Cl:N molar ratio of 1.5:1, as well as 2.0 mW/cm $^2$  of LPUV irradiance. The results are shown in Figures 3.7-3.9.

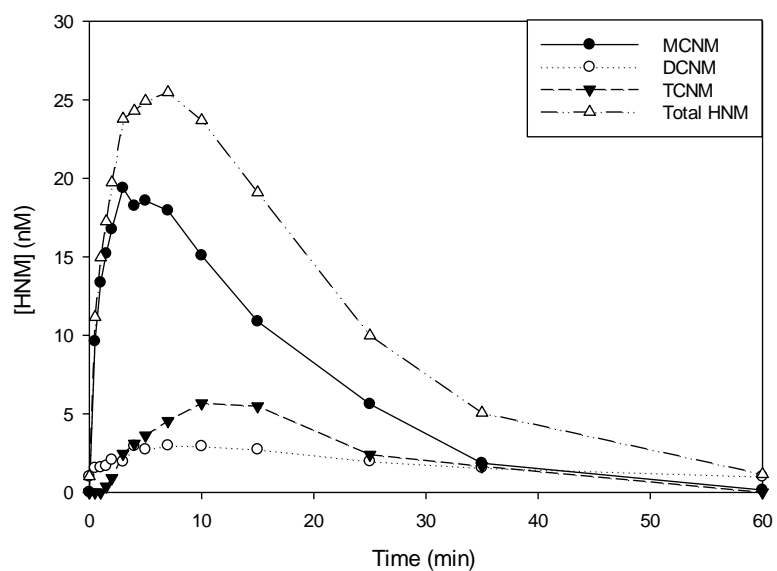


**Figure 3.7:** HNM formation from MA as a precursor under combined UV/Cl<sub>2</sub>. [MA]<sub>0</sub> = 73 μM, [FAC]<sub>0</sub> = 7.75 mg/L, 2 mW/cm<sup>2</sup> LPUV irradiance, pH 7.0, and 22 °C, n=1.

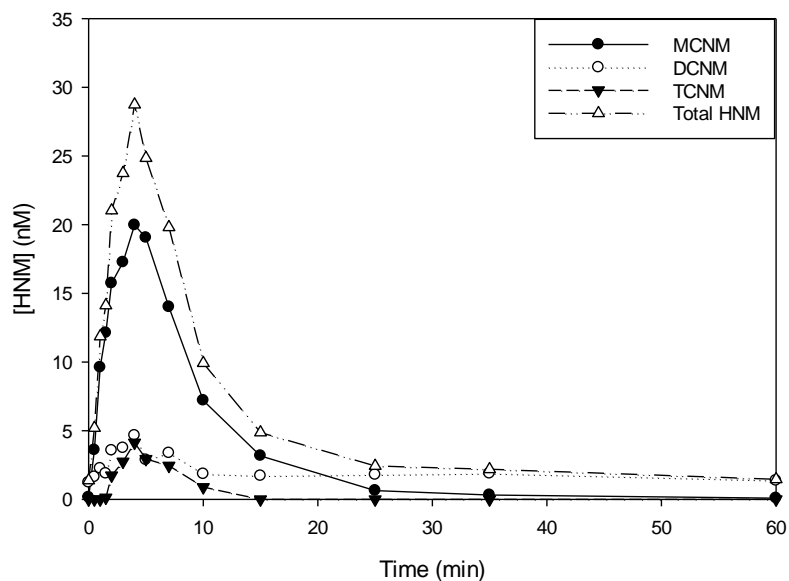


**Figure 3.8:** HNM formation from DMA as a precursor under combined UV/Cl<sub>2</sub>. [DMA]<sub>0</sub> = 73 μM, [FAC]<sub>0</sub> = 7.75 mg/L, 2 mW/cm<sup>2</sup> LPUV irradiance, pH=7.0, and 22 °C, n=1.

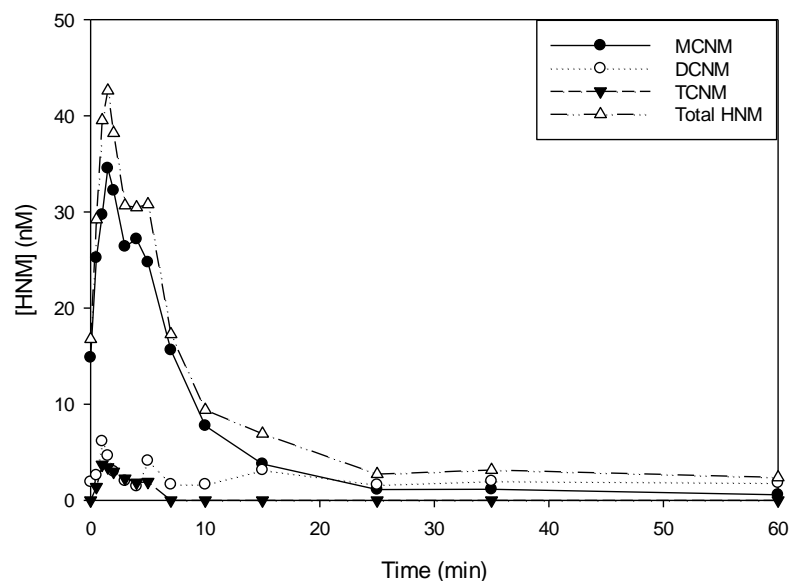


**Figure 3.9:** HNM formation from Gly as a precursor under combined UV/Cl<sub>2</sub>. [Gly]<sub>0</sub> = 73 μM, [FAC]<sub>0</sub> = 7.75 mg/L, 2 mW/cm<sup>2</sup> LPUV irradiance, pH=7.0, and 22 °C, n=1.

In each precursor case, MCNM formed in a higher concentration compared to the other HNMs. When MA was used (Figure 3.7), the peak MCNM concentration was at 19.4 nM, followed by TCNM at 5.7 nM, and DCNM at 3.0 nM. When DMA was the nitrogenous precursor, a similar trend of MCNM, DCNM, and TCNM at 20.0, 4.6, and 4.1 nM, respectively, was observed (Figure 3.8). Glycine was the strongest precursor, forming the most amounts of HNMs with MCNM followed by DCNM and TCNM at 34.6, 6.1, and 3.7 nM, respectively (Figure 3.9). In contrast, Table 3.2 shows there was no detectable HNMs formed from lysine as a precursor. Lysine has two nitrogens, with one on the end of the long chain aliphatic tail ( $\epsilon$ -carbon) and the other located on the  $\alpha$ -carbon (Table 1.2). The  $\epsilon$ -carbon-nitrogen bond is expected to be much more reactive than the  $\alpha$ -carbon-nitrogen bond to chlorine and possibly radicals, thus not reacting in similar HNM formation pathways.

**Table 3.2:** Lysine Peak Areas in the presence and absence of UV.

| Chemical | Minimum Detectable Peak Area | Max Peak Area (w/ UV) | Max Peak Area (w/o UV) |
|----------|------------------------------|-----------------------|------------------------|
| MCNM     | 748433.5                     | 38578                 | 6326                   |
| DCNM     | 274172.9                     | 9276                  | 16776                  |
| TCNM     | 246956.9                     | 39102                 | 41819                  |

### 3.5 Radical Quenching

#### 3.5.1 Tert Butyl Alcohol

*Tert*-butyl alcohol (TBA) was used due to its ability to quench both halogen and hydroxyl radicals rapidly (Gilbert et al 1988), which can form from the combined UV/Cl<sub>2</sub> system. TBA was added at 1 g/L to 73  $\mu$ M MA and 7.75 mg/L FAC (Cl:N = 1.5:1) to determine the effects of these radicals under the combined UV/Cl<sub>2</sub> system as well as in a similar system in the absence of UV. Figure 3.10 shows the maximum concentrations at 3.2, 0.5, 12.6 nM for MCNM, DCNM, and TCNM respectively. Compared to Figure 3.7 under similar reaction conditions but without TBA, there were a decrease in individual and total HNM formation and an inverted trend of MCNM and TCNM, where TCNM became the predominant form of HNM formation in contrast to the predominance of MCNM in the reaction without addition of TBA. Similarly, at lower TBA doses of 0.5, 0.1, and 0.01 g/L, similar trends were observed but at smaller quantities of Total HNM comprising of 90% or more TCNM in both new cases, shown in Figure 3.11 below.

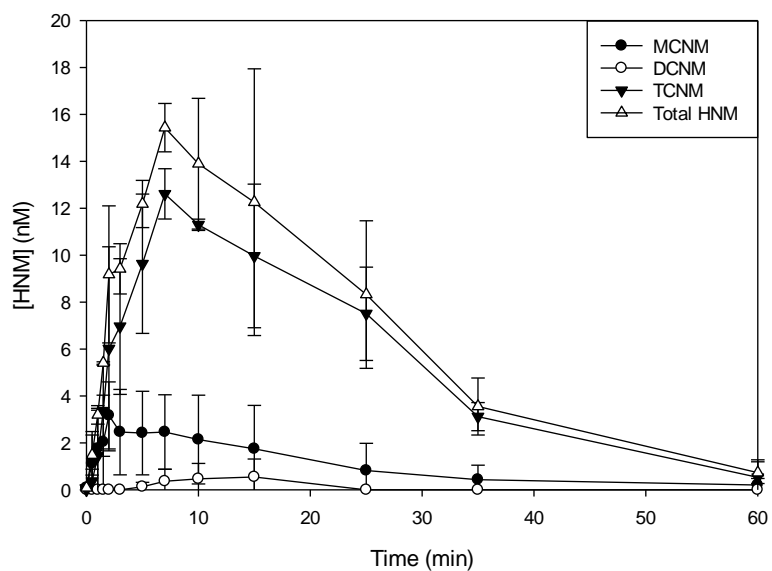


**Figure 3.10:** HNM formation from MA under combined UV/Cl<sub>2</sub> with the addition of 1 g/L TBA. [MA]<sub>0</sub> = 73 μM, [FAC]<sub>0</sub> = 7.75 mg/L, 2 mW/cm<sup>2</sup> LPUV irradiance, pH 7.0 and 22 °C, error bars are standard deviation, n=2

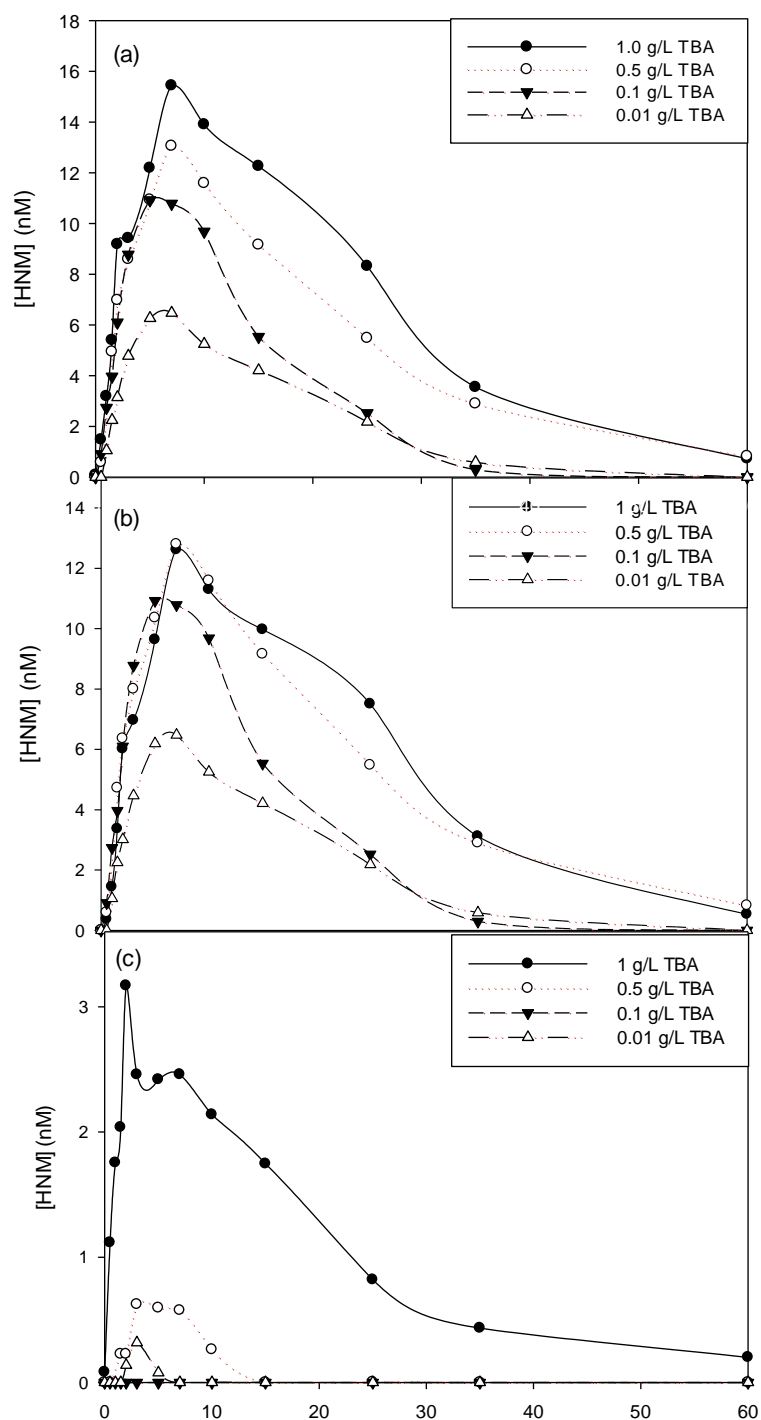


**Figure 3.11:** a) Total HNM, (b) TCNM, and (c) MCNM formation from MA under combined UV/Cl<sub>2</sub> with addition of varying amounts of TBA. [MA]<sub>0</sub> = 73 μM, [FAC]<sub>0</sub> = 7.75 mg/L, 2 mW/cm<sup>2</sup> LPUV irradiance, pH 7.0, and 22 °C, n=1

### 3.5.2 Sodium Acetate

Acetate anions can react with halogen radicals ( $\text{Cl}\cdot$ ) 50 times faster than with hydroxyl radicals ( $\text{OH}\cdot$ ) (Buxton et al 2000), which both form from the combined UV/ $\text{Cl}_2$  system. Sodium acetate was added at 1 g/L to 73  $\mu\text{M}$  MA and 7.75 mg/L FAC ( $\text{Cl}:\text{N} = 1.5:1$ ) as an attempt to differentiate the effects of  $\text{Cl}\cdot$  versus  $\text{OH}\cdot$  under the combined UV/ $\text{Cl}_2$  system. Figure 3.12 shows the maximum concentrations at 2.3, 6.0, and 24.1 nM for MCNM, DCNM, and TCNM respectively. Compared to Figure 3.7 under similar reaction conditions but without acetate, there was actually a small increase in the total HNM concentration, and an inverted trend of MCNM and TCNM, where TCNM was in much greater concentration than MCNM, in contrast to the reaction without the addition of acetate. In addition, with sodium acetate, there was more DCNM detected compared to experiments which lacked sodium acetate. These results imply that the halogen radical inhibits DCNM and TCNM formation since these species were detected at higher quantities when less  $\text{Cl}\cdot$  were available.

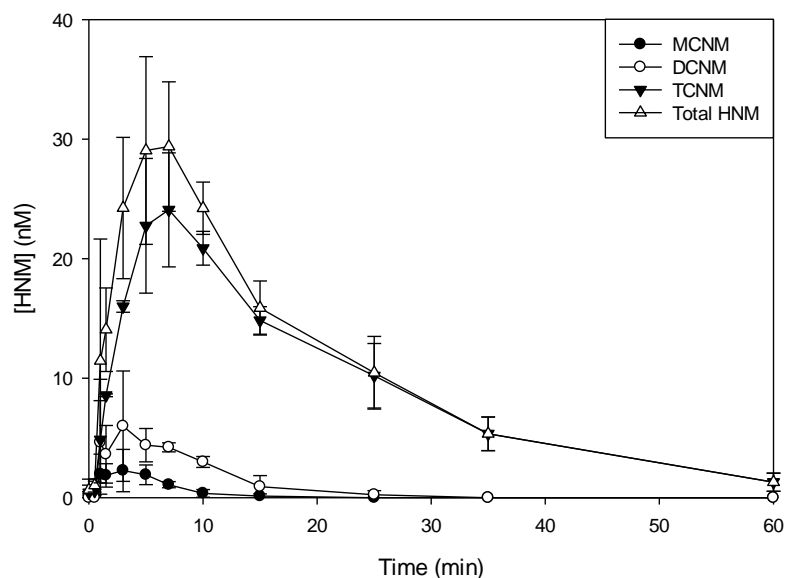


**Figure 3.12:** HNM formation from MA under combined UV/Cl<sub>2</sub> conditions with addition of 1.0 g/L of sodium acetate. [MA]<sub>0</sub> = 73 μM, [FAC]<sub>0</sub> = 7.75 mg/L, 2 mW/cm<sup>2</sup> LPUV irradiance, pH 7.0, and 22 °C, error bars are standard deviation, n=3

### 3.5.3 Nitrobenzene

Nitrobenzene reacts with OH• relatively fast ( $k = 3.9 \times 10^9 \text{ M}^{-1}\text{s}^{-1}$ ) while remaining unreactive with Cl• (Watts et al. 2007). NB was added at 0.05 g/L to 73 μM MA and 7.75 mg/L FAC (Cl:N = 1.5:1) as an attempt to differentiate the effects of Cl• versus OH• under the combined UV/Cl<sub>2</sub> system. Figure 3.13 shows NB affecting a continuous growth of HNM formation throughout the experiment duration. It was believed that NB might be a suitable nitrogenous precursor for HNM formation. In Figure 3.14 similar experiments were used as in Figure 3.13, with the lack of MA, to prove NB is a HNM nitrogenous precursor under a combined UV/Cl<sub>2</sub> system. It should be noted that HNM concentration went up to 90 nM, which was reached within 10-15 min. However, these NB-involved reactions were the only cases to reach such high concentrations of HNMs and thus it is reasonable to believe NB is a significant HNM precursor.



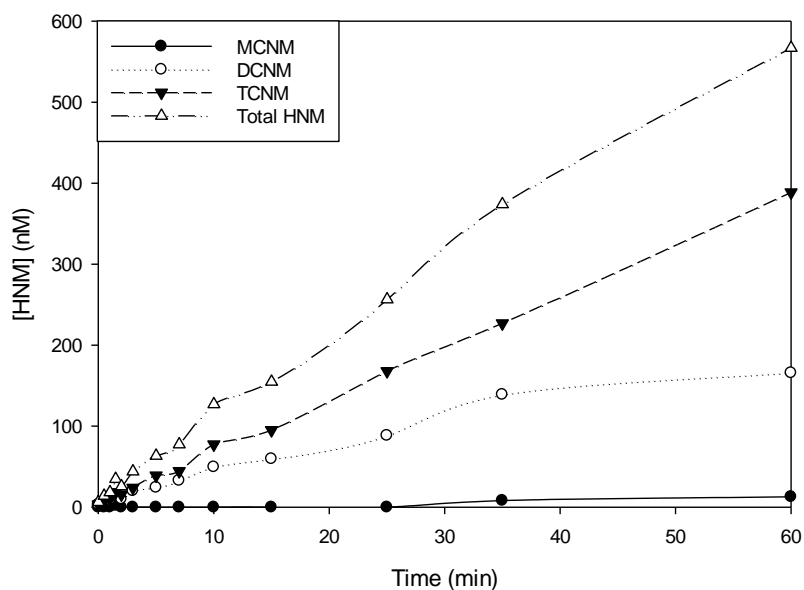


**Figure 3.13:** HNM formation from MA under combined UV/Cl<sub>2</sub> conditions with addition of 0.05 g/L of NB. [MA]<sub>0</sub> = 73 μM, [FAC]<sub>0</sub> = 7.75 mg/L, 2 mW/cm<sup>2</sup> LPUV irradiance, pH 7.0, and 22 °C.

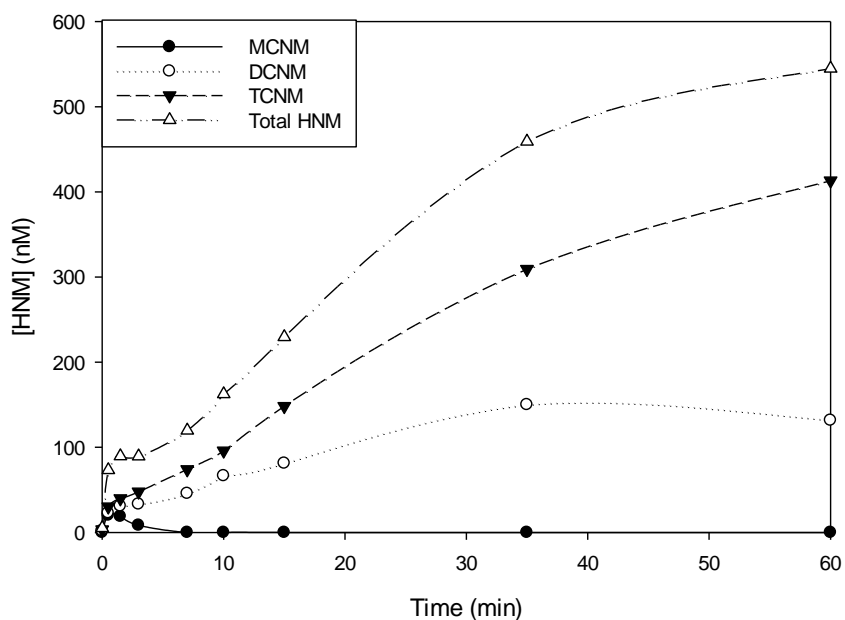


**Figure 3.14:** HNM formation under combined UV/Cl<sub>2</sub> conditions with addition of 0.05 g/L of NB. [MA]<sub>0</sub> = 0 μM, [FAC]<sub>0</sub> = 7.75 mg/L, 2 mW/cm<sup>2</sup> LPUV irradiance, pH 7.0, and 22 °C.

## 3.6 Real Waters

### 3.6.1 Wastewater Sample

Effluent from a local domestic wastewater treatment plant was collected after membrane filtration and prior to any type of disinfection. Chlorine demand of the wastewater sample after 10 min was found to be 4.2 mg/L. The chlorine demand of DI water with 73  $\mu$ M MA was around 4.7 mg/L. To maintain constant chlorine residual levels of 3.0 m/L in both sample matrices, initial chlorine of 7.25 mg/L was added to the unaltered wastewater matrix and initial chlorine of 11.3 mg/L was added into the wastewater matrix spiked with 73  $\mu$ M MA. Figure 3.15 shows the formation of HNMs in the unmodified wastewater effluent sample from UV/Cl<sub>2</sub> exposure. Since the wastewater sample underwent membrane filtration prior to collection, it is likely a high amount of nitrogenous precursors were removed compared to other wastewater samples studied (Fang et al 2013). In this case, DCNM peaked at 2.8 nM, TCNM peaked at 2.3 nM, and total HNM peaked at 5.1 nM. There was no detectable MCNM. Figure 3.16 shows HNM formation when 73  $\mu$ M of MA was spiked into the wastewater matrix. There was a total decrease of HNM formation. Maximum TCNM concentration was 5.5 nM followed by 3.8 nM of DCNM, and a total HNM peak at 9.2 nM. There was no detectable MCNM formation.

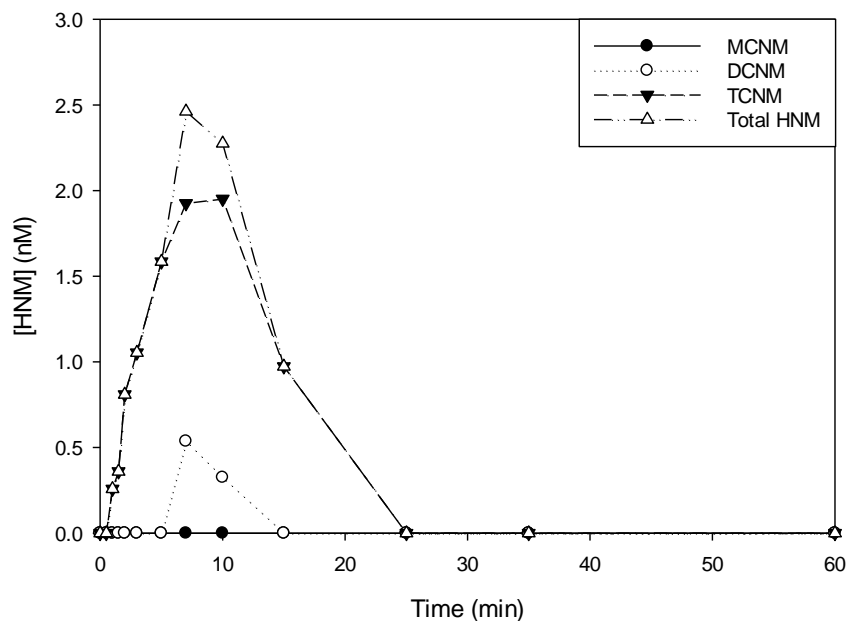


**Figure 3.15:** HNM formation from a wastewater sample under combined UV/Cl<sub>2</sub> conditions. [FAC]<sub>0</sub> = 7.25 mg/L, 2 mW/cm<sup>2</sup> LPUV, pH 7.0, and 22 °C, n=1.

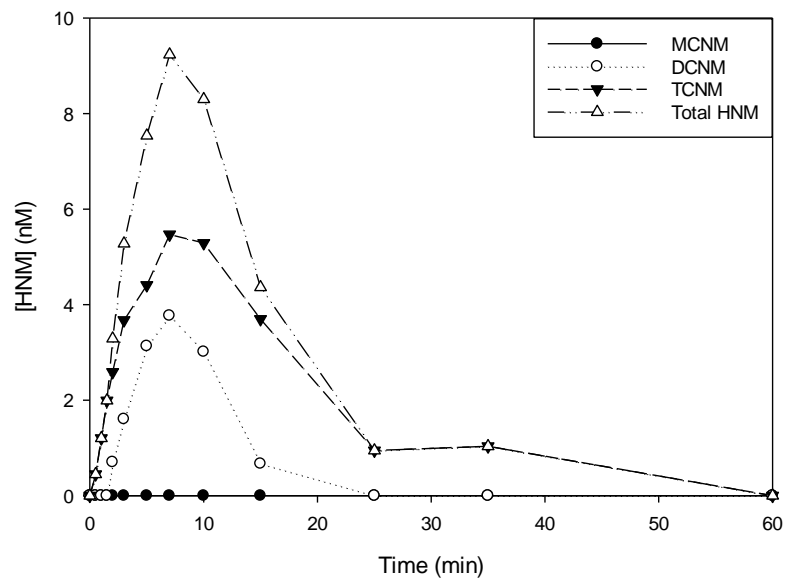


**Figure 3.16:** HNM formation from a wastewater sample spiked with 73 μM MA under combined UV/Cl<sub>2</sub> conditions. [FAC]<sub>0</sub> = 11.3 mg/L, 2 mW/cm<sup>2</sup> LPUV, pH 7.0, and 22 °C, n=1.

### 3.6.2 River Water Sample

Water from the Chattahoochee River near Atlanta was collected and used as a representative surface water matrix. The river water had a chlorine demand of 2.1 mg/L, and to maintain a 3 mg/L free chlorine residual, 5.1 mg/L of chlorine dose was used in the unaltered river water matrix and 9.8 mg/L of chlorine dose in the river water matrix spiked with 73  $\mu\text{M}$  MA. Figure 3.17 shows the formation of HNMs in the unmodified river water under combined UV/ $\text{Cl}_2$  conditions. TCNM peaked followed by DCNM and MCNM at 12.7 nM, 11.0 nM and 9.7 nM, respectively (Total HNM = 33.4 nM). Figure 3.18 shows HNM formation when 73  $\mu\text{M}$  of MA was spiked into the river water matrix under UV/ $\text{Cl}_2$ . Maximum DCNM concentration was 3.9 nM, followed by MCNM (8.6 nM), and TCNM (14.4 nM,) for a total HNM peak at 26.8 nM.

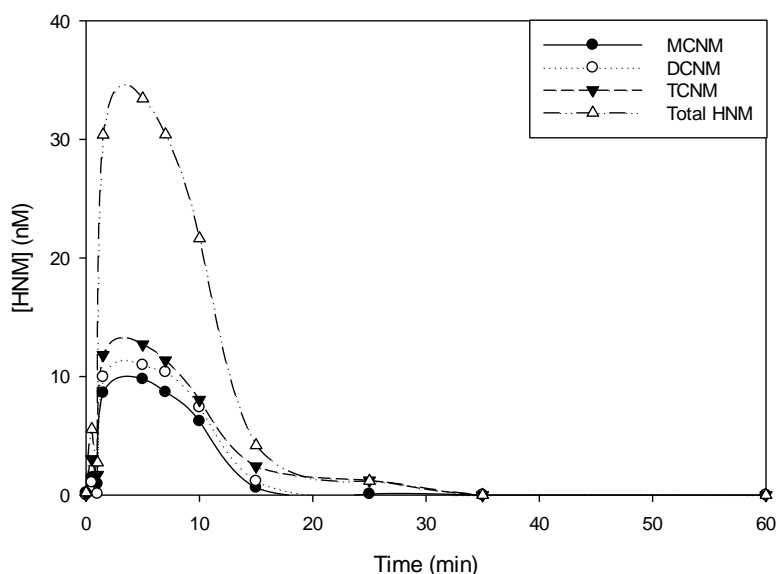


**Figure 3.17:** HNM formation from river water under combined UV/ $\text{Cl}_2$  conditions.  $[\text{FAC}]_0 = 5.10 \text{ mg/L}$ ,  $2 \text{ mW/cm}^2 \text{ LPUV}$ , pH 7.0, and  $22^\circ\text{C}$ ,  $n=1$ .

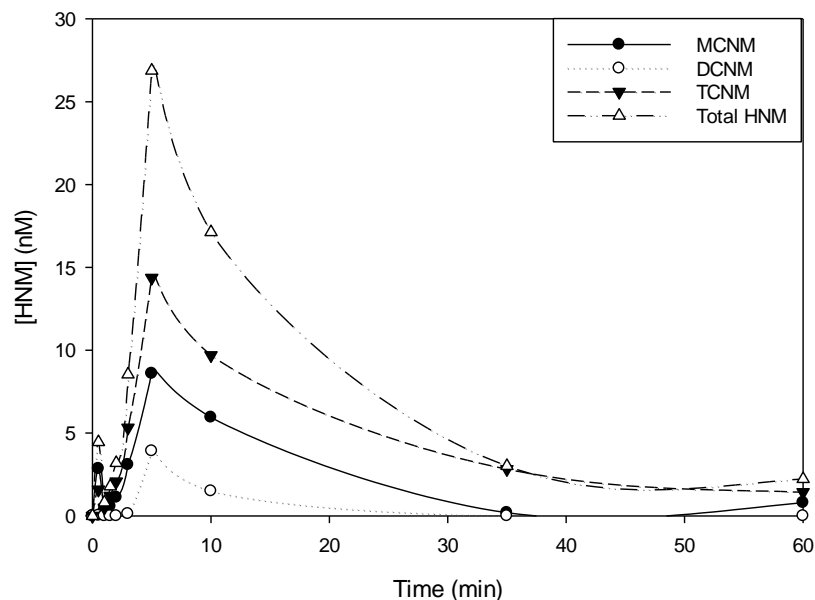


**Figure 3.18:** HNM formation from river water spiked with 73  $\mu\text{M}$  MA under combined UV/ $\text{Cl}_2$  conditions.  $[\text{MA}]_0=$ ,  $[\text{FAC}]_0= 9.8 \text{ mg/L}$ ,  $2 \text{ mW/cm}^2$  LPUV, pH 7.0, and  $22^\circ\text{C}$ ,  $n=1$ .

### 3.6.3 Partially Treated Drinking Water Sample

Water was collected after coagulation and flocculation and prior to any disinfection from a drinking water treatment plant with source water from the Lake Alatoona in Georgia. The chlorine demand of the drinking water sample was determined to be 1.5 mg/L after 10 min. To maintain a 3.0 mg/L chlorine residual, 4.5 mg/L chlorine was added in the unaltered drinking water and 9.2 mg/L free chlorine was added in the drinking water spiked with 73  $\mu\text{M}$  MA. Figure 3.19 shows the HNM formation from the unaltered drinking water exposed to UV/ $\text{Cl}_2$ . TCNM and DCNM peaked at 1.7 and 1.1 nM, respectively (total 2.8 nM), while no MCNM could be detected. Figure 3.20 shows the HNM formation from the drinking water spiked with 73  $\mu\text{M}$  MA; TCNM and DCNM peaked at 3.7 nM and 3.1 nM, respectively (total HNM = 6.8 nM) and no MCNM could be detected.

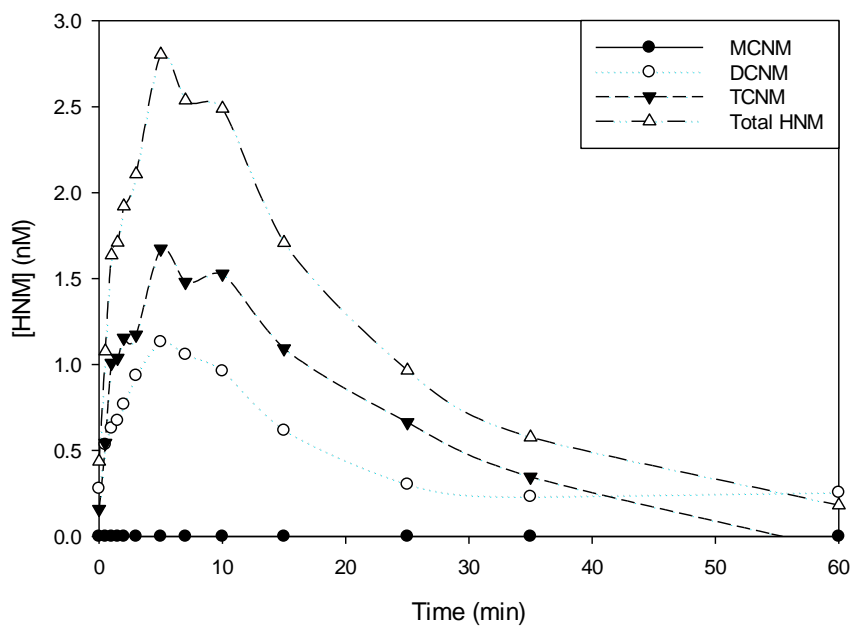


**Figure 3.19:** HNM formation from partially treated drinking water under combined UV/Cl<sub>2</sub> conditions. [FAC]<sub>0</sub>= 4.5 mg/L, 2 mW/cm<sup>2</sup> LPUV, pH 7.0, and 22 °C, n=1.

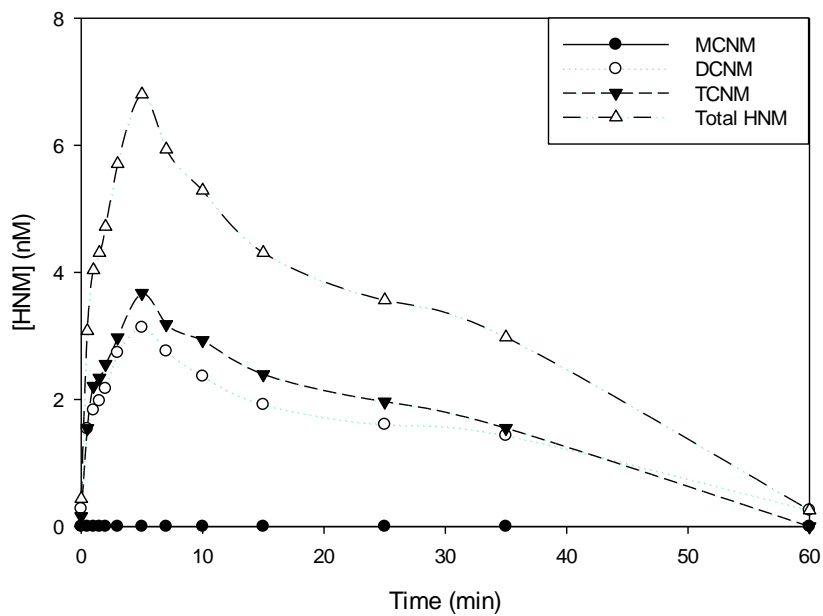


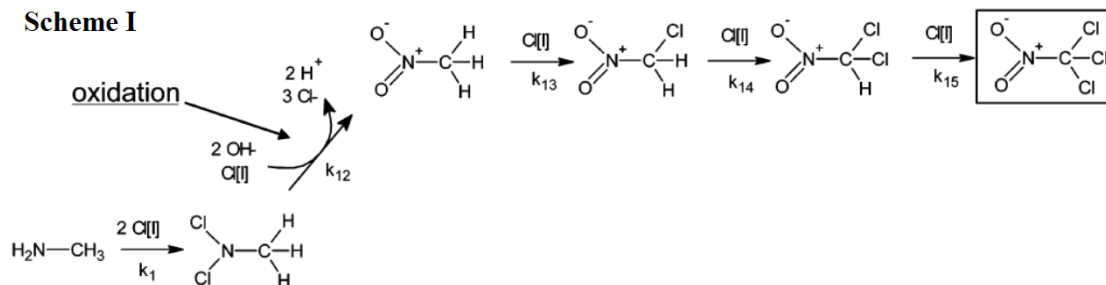
**Figure 3.20:** HNM formation from partially treated drinking water spiked with 73 μM MA under combined UV/Cl<sub>2</sub> conditions. [FAC]<sub>0</sub>= 9.2 mg/L, 2 mW/cm<sup>2</sup> LPUV, pH 7.0, and 22 °C, n=1.

In each of the above real water cases, Figures 3.15-20, the HNM concentration peak lasted longer in time compared to the HNM formation in DI water matrices (Figure 3.7), suggesting more gradual formation and more gradual decay of HNMs in the real water samples. This can be partly attributed to additional different nitrogenous precursors present in the real waters. In addition, constituents in the real waters may absorb or scatter the incoming UV light, causing the decrease in HNM formation and slower decay rates compared to those in DI water. Moreover, the trend of distribution among MCNM, DCNM and TCNM in the real water matrices differed significantly from that in the DI water matrix, most significantly with switching from MCNM dominance in the DI water to TCNM dominance in the real waters. The dominance of TCNM among HNMs in real water samples is consistent with previous research that has studied HNMs' occurrence/formation in real water samples or water/wastewater treatment systems. The mechanism for this trend, however is unclear. Thus, more research is needed to better understand the impact of real water matrices on the HNM formation under chlorination as well as combined UV/Cl<sub>2</sub> conditions.

### **3.7 Reaction Mechanisms**

#### **3.7.1 Formation of HNMs by Chlorination**

Joo and Mitch have proposed a mechanism of MCNM, DCNM, and TCNM formation in systems where chlorination or chloramination of MA occurs (Scheme I below). It involves rapidly forming a dichloroamine from MA, followed by oxidation into a nitroalkane. Once the nitroalkane is formed, chlorination of the alkane occurs with the first chlorination being the rate-limiting step (Fang et al 2013) due to increased acidity from electron-withdrawing chlorines (Joo and Mitch 2007).

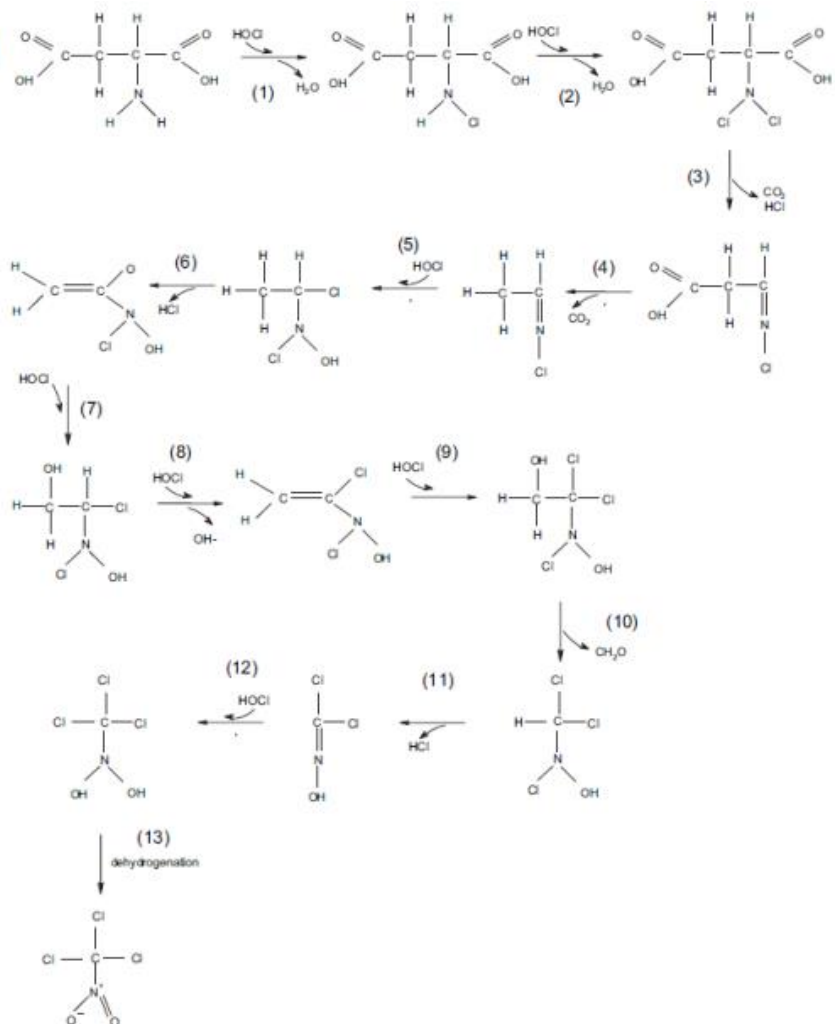


Scheme I: Proposed HNM formation under chlorination, Joo and Mitch 2007.

Hu and colleagues studied the formation potentials of CNMs and proposed a formation mechanism of TCNM from aspartic acid, an amino acid (Hu et al 2010a). Again, the first step is chlorination of the amine group (reactions 1-2). Since glycine is a smaller compound than aspartic acid, not as much  $\text{CO}_2$  will be released and can differ in reaction processes 3-7. The 2 sole carbons in glycine can form double bonds from  $\text{HOCl}$  and eliminate the one carbon through  $\text{CH}_2\text{O}$  (Reactions 8 and 9). It would be followed by formation of C-N double bond, oxidation of C-N bond by  $\text{HOCl}$ , and dehydrogenation of the N hydroxyl groups forming TCNM.



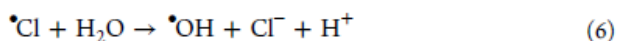
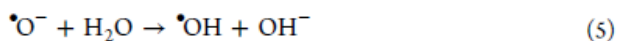
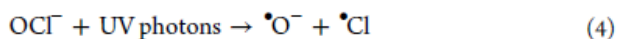
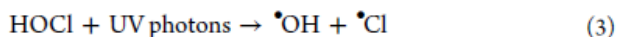
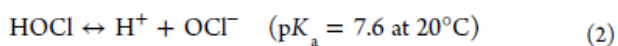
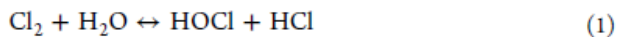
**Scheme II**



Scheme II: HNM formation from aspartic acid under chlorination (Hu et al 2010a).

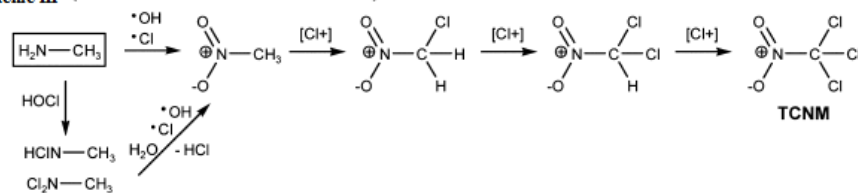
### 3.7.2 Formation of HNMs under combined UV/Chlorine Conditions

In a combined UV/Chlorine system, previous studies (Deng et al 2014, Jin et al 2011) have shown the following reactions can occur to generate OH and Cl radicals:

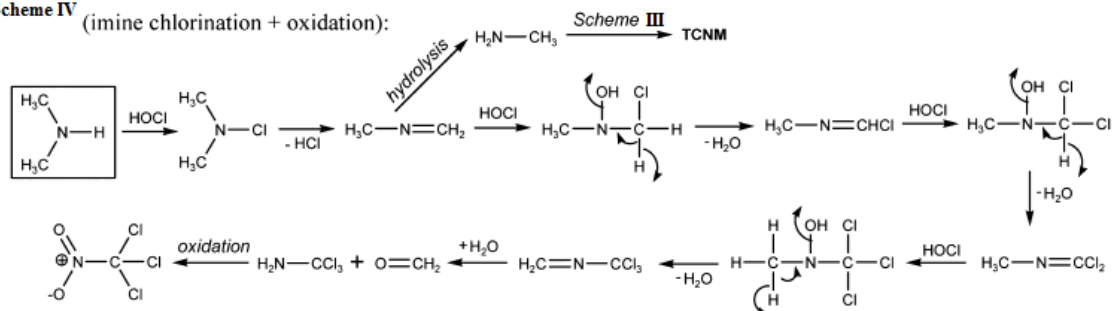


The photolysis of HOCl can lead to production of OH<sup>•</sup> and Cl<sup>•</sup> (reaction 6) and can perpetually create more radicals (reaction 5-7). Schemes III and IV below have been suggested by Deng et al. (2014) and show how the radicals react with the nitrogenous precursors forming HNMs. Scheme III illustrates a simple amine precursor, such as MA or glycine, and their reaction with OH<sup>•</sup> and Cl<sup>•</sup> radicals, oxidizing the amine group to a nitro group. It is then followed by sequential halogenation of the methyl group, resulting in MCNM, DCNM, or TCNM. Scheme IV shows the formation from secondary amines such as DMA. DMA reacts with free chlorine to create a methyl-imine intermediate which can undergo two mechanisms. It can undergo hydrolysis yielding MA and follow Scheme III. Alternatively, the intermediate can continue chlorination forming a trichloromethylamine, followed by oxidation of the amine into a nitro group (Deng et al 2014, Hu et al 2010a).

**Scheme III** (radical oxidation + chlorination):



**Scheme IV** (imine chlorination + oxidation):



Scheme III and IV: HNM formation from UV radicals and chlorination (Deng et al 2014)

## **CHAPTER 4**

### **CONCLUSIONS AND RECOMMENDATIONS**

#### **4.1 Conclusion**

The results from this study show how different precursors affect HNM formation as well as how different free chlorine doses can affect HNM speciation. This study shows that the LPUV and free chlorine concurrent exposure can enhance HNM formation. In addition to chlorination reactions, there are other types of reactions involved in the combined UV/Cl<sub>2</sub>, such as radical reactions and photoreaction. The radical reactions can include OH<sup>•</sup>, Cl<sup>•</sup>, and other unidentified radicals that can lead to oxidation of the amino group to a nitro group (Deng et al. 2014) or other reactions. Photoreactions include chloramines from chlorinated nitrogenous precursors, photodecay of HNMs, and other unknown photoreactions of reaction intermediates.

In addition, most previous studies showed TCNM forming in greater quantities followed by MCNM and DCNM. However, the results of this study show that, in DI water matrices, MCNM forms in greater quantities at Cl:N ratios less than three, while TCNM forms in greater quantities at Cl:N ratios greater than three. Even so, the increase in TCNM formation did not increase linearly as the Cl:N ratio increased; there was a decreased rate of return when Cl:N ratios were greater than three.

The type of nitrogenous precursors can affect the amount of HNMs formed, with glycine forming a higher amount of total HNMs compared to MA and DMA. The source of water can also affect which HNM species is formed in greater concentrations. The limited number of real water samples showed that the river waters have higher than normal TOC and DON, which are associated with greater nitrogenous precursors and higher HNM formation.

Results from the radical quencher experiments indicate the reaction mechanisms are highly complex. Radical species are an important factor in determining the formation mechanism but it was difficult to determine their reaction pathways or specific roles based on the experimental outcomes. More research is needed in this area.

The real water experiments show the formation of CNMs is even more complex in real water matrices. Real waters can contain factors that are not present in the DI water matrices, which altered reaction intermediates and pathways. These altered reactions resulted in different levels of total HNMs as well as different abundance distribution among MCNM, DCNM, and TCNM. There is a significant contrast in outcomes where MCNM is the dominant CNM formed in DI water matrices, whereas TCNM is the dominant CNM formed in real water matrices. The dominance of TCNM formation in real water samples is consistent with previous research that has surveyed and studied HNM DBPs in real water samples or systems (Bond et al. 2012). Each water source can have different nitrogenous precursors; river waters may have more algal organic matter while wastewater would have higher organic matter and synthetic chemicals. In addition, source waters can have different constituents, such as varying DO levels and inorganic ions, which might inhibit HNM formation or affect speciation.

## **4.2 Recommendations**

Future studies should vary the UV irradiance and radical quenching doses to determine if the radicals' role changes with changing UV irradiance. Additionally, determining the type of nitrogenous precursors in real waters can help understand the kinetics and levels of HNM formation; the simple MA formed HNMs at a slower rate compared to DMA and Gly. Additional studies on the brominated nitromethanes need to be done, since these have greater genotoxicity and cytotoxicity compared to CNMs. More research is needed to better understand the impact of real water matrices on the HNM formation under chlorination as well as combined UV/Cl<sub>2</sub> conditions in general.

## REFERENCES

- Bolton, JR. *Ultraviolet Applications Handbook* 3<sup>rd</sup> ed. ICC Lifelong Learn Inc. Edmonton Canada. 2010.
- Bond, T., Huang, J., Templeton, MR., Graham, N.; *Occurrence and control of nitrogenous disinfection by-products in drinking water. A review.* Water Research. 2011. 45, 4341-4354
- Bond, T., Templeton, MR., Graham, N. *Precursors of nitrogenous disinfection by-products in drinking water A critical review and analysis.* Journal of Hazardous Materials. 2012. 1-16
- Buxton, GV., Wang, J., Salmon, GA. *Rate constants for the reactions  $NO_3^\bullet$ ,  $SO_4^\bullet$  and  $Cl^\bullet$  radicals with formate and acetate esters in aqueous solution.* Phys. Chem. 2001, 3, 2618-2621
- Cantor, KP. *Drinking water and Cancer.* Cancer Causes and Control. 1997, 8, 292-308
- Cole, S.K., Cooper, W.J., Fox, R.V., Gardinali, P.R., Mezyk, S.P., Mincher, B.J., O'Shea, K.E. *Free radical chemistry of disinfection byproducts 2. Rate constants and degradation mechanism of TCNM.* Environmental Science and Technology. 2007, 41, 863-869.
- Corin, N., Backlund, P., Kulovaara, M., *Degradation products formed during UV-irradiation of humic waters.* Chemosphere 1996. 33, 245-55
- Craik, SA., Weldon, D., Finch, GR., Bolton, JA., Belosevic, M.: *Inactivation of cryptosporidium parvum oocysts using medium- and low- pressure ultraviolet radiation.* Water Research. 2001. 35, 1387-1398
- Deng, L., Huang, CH., Wang, YL. *Effects of combined UV and chlorine treatment on the formation of trichloronitromethane from amine precursors.* Env. Sci. Tech. 2014. 48, 2697-2705.

- Dotson, AD., Rodriguez, CE., Linden, KG. *UV disinfection implementation status in United States water treatment plants*. Journal of the American Water Works Association, 2012. 104, E318-E324.
- Fang JY., Ling, L., Shang, C. *Kinetics and mechanisms of pH dependent degradation of HNM by UV Photolysis*. Water Research. 2013. 47, 1257-1266
- Feng, YG., Smith, DW., Bolton, JR., *Photolysis of aqueous free chlorine species with 354 nm ultraviolet light*. Journal of Environmental Engineering and Sciences. 2007. 3, 277-284
- Gilbert, B. C.; Stell, J. K.; Peet, W. J.; Radford, K. J. *Generation and reactions of the chlorine atom in aqueous solution*. J. Chem. Soc. Faraday Trans. 1988. 84, 319-3330.
- Hijnen, WAM., Beerendonk, EG., Medema, GJ. *Inactivation credit of UV radiation for viruses, bacteria and protozoan (oo)cysts in water: a review*. Water Research. 2006. 40 (1), 3-22
- Hodgeson, JW., Cohen, AL. *Method 551, Determination of chlorination disinfection byproducts and chlorinated solvents in drinking water by liquid-liquid extraction and gas chromatography with electron-capture detection*. EPA. 1990.
- Hrudey, SE. *Chlorination disinfection by-products, public health risk tradeoffs and me*. Water Research. 2009. 43, 2057-2092
- Hu, J., Song, H., Addison, J.W., Karanfil, T. *Halonitromethane Formation potentials in drinking waters*. Water Research. 2010a. 44, 105-114.
- Hu, J., Song, H., Karanfil, T. *Comparative analysis of Halonitromethan and trihalomethane formation and speciation in drinking water: The effects of disinfectants, pH, bromide, and nitrite*. Env. Sci. and Tech. 2010b. 44, 794-799

Huang, FQ., Ruan, MY., Yan, JD., Hong, HC., Lin, HJ., Xiong, YJ. *An improved method for determining HNMs in drinking water*. 2013, Water Science and Technology, 13.5, 1257-1264.

Jin J., El-Din, M.G., Bolton, J.R. *Assessment of the UV/Chlorine process as an advanced oxidation process*. Water Research. 2011. 45, 1890-1896

Joo, SH., Mitch, WA. *Nitrile, aldehyde, and halonitroalkane formation during chlorination/chloramination of primary amines*. Environmental Science and Technology. 2007, 41, 1288-1296.

Krasner, S.W., Weinberg, HS., Richardson SD., Pastor SJ., Chinn, R., Scilimenti, MJ., Onstad, GD., Thruston, AD. *Occurrence of a new generation of disinfection byproducts*. Environmental Science and Technology. 2006, 40, 7175-7185

Korshin, GV., Benjamin, MM., Chang, HS., Gallard, H. *Examination of NOM chlorination reactions by conventional and stop-flow differential absorbance spectroscopy*. Environmental Science and Technology. 2007. 41(8), 2776-81

Li, J., Blatchley, ER. *UV Photodegradation of inorganic chloramines*. Environmental Science and Technology. 2009, 43

Liu, W., Zhang, Z., Yang, X., Xu, Y., Liang, Y. *Effects of UV irradiation and UV/Chlorine co exposure on natural organic matter in water*. Science of the Total Environment 2012. 414, 576-584

Lyon, BA., Dotson, AD., Linden, KG., Weinberg, HS. *The effect of inorganic precursors on disinfection byproduct formation during UV-chlorine/chloramine drinking water treatment*. Water Research. 2012. 46, 4653-4664

Mezyk, S.P., Helgeson T., Cole, SK., Cooper, WJ., Fox, RV., Gardinali, PR., Mincher, BJ. *Free radical chemistry of disinfection byproducts 1) Kinetics of hydrated electron and hydroxyl reactions with halonitromethanes in water*. Journal of Physical Chemistry. 2006. 110, 2176-2180



Mincher, B.J., Mezyk, S.P., Cooper, W.J., Cole, S.K., Fox, R.B., Gardinali, P.R. *Free Radical chemistry of disinfection byproducts 3. Degradation mechanism of Chloronitromethane, Bromonitromethane, and dichloronitromethane*. Journal of Physical Chemistry. 2010, 114, 117-125

Mitch, W.A., Krasner, S.W., Westerhoff, P., Dotson, A., *Occurrence and formation of nitrogenous disinfection by-products*. Water Research Foundation, Denver, CO, US, 2009.

Montemayor, M., Costan, A., Lucena, F., Jofre, J., Muñoz, J., Dalmau, E., Mujeriego, R., Sala, L. *The combined effects of UV light and chlorine during reclaimed water disinfection*. Water Science and Technology. 2008. 57.6, 935-940.

Nieuwenhuijsen, M.J., Toledano, M.B., Elliott, P. *Uptake of chlorination disinfection by-products; a review and discussion of its implications for exposure assessment in epidemiological studies*. Journal of Exposure Analysis and Environmental Epidemiology. 2000. 10, 586-599.

Plewa, M.J., Wagner, E.D., Jazwierska, P. *Halonitromethane Drinking water disinfection byproducts: Chemical Characterization and mammalian cell cytotoxicity and genotoxicity*. Environmental Science and Technology. 2004. 38, 62-68

Pontius, F.W. *Water Quality and Treatment*; McGraw-Hill, Inc.: New York, 1990; Chapter 1, pp 1-61

Richardson, S.D., Plewa, M.J., Wagner, E.D., Schoeny, R., DeMarini, D.M. *Occurrence, genotoxicity, and carcinogenicity of regulated and emerging disinfection byproducts in drinking water: a review and roadmap for research*. Mutation Research-Reviews in Mutation Research. 2007. 636 (1-3), 178-242.

Shah, A.D., Mitch, W.A. *Halonitroalkanes, Halonitriles, Haloamides, and N-Nitrosamines: A Critical Review of Nitrogenous Disinfection Byproduct Formation Pathways*. Environmental Science and Technology. 2012, 46, 119-131

- Shan, J et al. *Effects of pH, bromide, and nitrite on halonitromethane and trihalomethane formation from amino acids and amino sugars*. Chemosphere. 2012. 86, 323-328.
- Villanueva, CM., Cantor, KP., Grimalt, JO., Malats, N. *Bladder Cancer and exposure to water disinfection by-products through ingestion, bathing, showering and swimming in pools*. American Journal of Epidemiology. 2007. 165, 148-156.
- Watts, MJ., Linden, KG. *Chlorine photolysis and subsequent OH radical production during UV treatment of chlorinated water*. Water Research. 2007. 41, 2871-2878.
- Weinberg, H.S., Krasner, S.W., Richardson, S.D., Thruston Jr., A.D. *The Occurrence of Disinfection By-products (DBPs) of Health Concern in Drinking Water: Results of a Nationwide DBP Occurrence Study*. EPA. 2002. 600/R-02/068.
- Weng, S., Li, J., Blatchley, E.R. *Effects of UV254 irradiation on residual chlorine and DBPs in chlorination of model organic-N precursors in swimming pools*. Water Research. 2012. 46, 2674-2682.
- Westerhoff, P., Mash, H., *Dissolved organic nitrogen in drinking water supplies: a review*. Journal of Water Supply Research and Technology. 2002. 51, 415-448.